mexR of the PAO4290 chromosome with two of the mutant *mexR* alleles described above. We used the most frequent *mexR* mutation described above that had a C to T substitution at nucleotide 73 (TNP030#10). Another mutation used was TNP030#11, which had an A to C substitution at nucleotide 388. We amplified *mexR* from these strains and replaced it with the homologous chromosomal gene in PAO4290. The nucleotide sequencing analysis of the chromosomal *mexR* of strain TNP078#10 showed a C to T substitution at nucleotide 73 as expected. Another mutant, TNP078#11, had two mutations: one was an A to C substitution as expected at nucleotide 388 and an additional T to G substitution at nucleotide 104. The latter mutation probably occurred accidentally during the course of the PCR amplification. Both *mexR* mutants carrying the impaired *mexR* showed a typical *nalB*-type antibiotic resistance profile, which was indistinguishable from that in TNP030#10 and TNP030#11 (Table 2). These *mexR* mutants also expressed the *mexA* transcriptional reporter comparable to that in the parent *nalB*-type mutants (Table 3). We concluded, based on these results, that the mutation in the *mexR* gene alone is sufficient to overexpress the *mexAB-oprM* operon and to confer *nalB*-type multi-antibiotic resistance in *P. aeruginosa*.

4. Discussion

The *mexAB-oprM* operon has been implicated as encoding the antibiotic efflux pump that is overexpressed in the *nalB*-type mutant [4], and the gene overcoming the iron utilization inhibitor, 2,2′-dipyridyl [3]. It has been assumed that the *nalB* locus encodes a regulator of the *mexAB-oprM* operon. More recently, the *mexR* gene was discovered upstream of the *mexAB-oprM* operon and the phenotype of the *mexR* mutation appeared to be similar to that of the *nalB* mutant [8]. Our data presented in this paper showed that all the *nalB*-type mutants isolated in this laboratory and one original *nalB9* mutant had a mutation at nine independent sites in the *mexR* gene. This finding is consistent with a previous analysis of the *mexR* gene of the *nalB*-type antibiotic-resistant strains isolated from clinical materials [9]. It must be stressed, however, that the sequencing analysis of the clinical isolates does not resolve the question of whether or not only the *mexR* mutation is sufficient to overexpress the MexAB-OprM efflux pump. To ascertain that no other mutation was involved in the expression of the *nalB* phenotype in our mutants, we replaced the mutant *mexR* with wild-type *mexR*. Furthermore, the wild-type *mexR* gene was replaced with previously characterized *nalB*-type *mexR* genes. The results obtained from these experiments support the notion that *mexR* is the only gene necessary to regulate expression of the *mexAB-OprM* operon. The next question to be addressed is whether or not *nalB* is identical to *mexR*.

We favor the notion that *nalB* is identical to *mexR* based on the following observations. In the earlier study, the *nalB9* mutation was mapped at 32 min of the *P. aeruginosa* (PAO6006) chromosome, which is close to *pyrB* and *proC* [5]. We searched the genome sequence database of *P. aeruginosa* and found that *mexR* is located between 174.5 and 175.0 kb of a 195.7-kb contig. The *pyrB* and *proC* genes were found at 146.3–148.5 kb and 138.4–139.1 kb, respectively. Therefore, the gene sequence on the database appeared to be *mexR-pyrB-proC*, which is exactly the same sequence of *nalB9-pyrB-proC* determined by previous transduction experiments [5]. These finding indicate that *nalB* and *mexR* are the same gene.

A recent paper reported that hyper-expression of the *mexAB-oprM* operon in the *nalB* strain cannot be explained simply by a null mutation in *mexR* and suggested the presence of an additional gene(s) [8,9]. Our paper does not rule out the possible presence of an upper regulator that acts on the *nalB/mexR* gene. However, it is not clear at present whether such an upper regulator is effective in the cell with the activated *mexR/nalB* gene. Since the identity of *nalB* and *mexR* has become clear, the designation of these genes should be coalesced. We propose to designate *nalB/mexR* as the *mexR* gene because of the designation of the operon to be regulated, which is *mexAB-oprM*.

Acknowledgements

This study was supported in part by grants from the Ministry of Education of Japan, Science, Sport

and Culture, the Ministry of Health and Welfare's Emerging and Re-emerging Infectious Diseases Program, the Japan Society for Promotion of Science, Tokai University School of Medicine's Project Research, and a Sasakawa Scientific Research Grant from The Japan Science Society.

References

[1] Nikaido, H. (1989) Outer membrane barrier as a mechanism of antimicrobial resistance. Antimicrob. Agents Chemother. 33, 1831–1836.

[2] Nakae, T. (1995) Role of membrane permeability in determining antibiotic resistance in *Pseudomonas aeruginosa*. Microbiol. Immunol. 39, 221–229.

[3] Poole, K., Krebes, K., McNally, C. and Neshat, S. (1993) Multiple antibiotic resistance in *Pseudomonas aeruginosa*: evidence for involvement of an efflux operon. J. Bacteriol. 175, 7363–7372.

[4] Morshed, S.R.M., Lei, Y., Yoneyama, H. and Nakae, T. (1995) Expression of genes associated with antibiotic extrusion in *Pseudomonas aeruginosa*. Biochem. Biophys. Res. Commun. 210, 356–362.

[5] Rella, M. and Haas, D. (1982) Resistance of *Pseudomonas aeruginosa* PAO to nalidixic acid and low levels of β-lactam antibiotics: mapping of chromosomal genes. Antimicrob. Agents Chemother. 22, 242–249.

[6] Lei, Y., Sato, K. and Nakae, T. (1991) Ofloxacin-resistant *Pseudomonas aeruginosa* mutants with elevated drug extrusion across the inner membrane. Biochem. Biophys. Res. Commun. 178, 1043–1048.

[7] Masuda, N. and Ohya, S. (1992) Cross-resistance to meropenem, cephems, and quinolones in *Pseudomonas aeruginosa*. Antimicrob. Agents Chemother. 36, 1847–1851.

[8] Poole, K., Tetro, K., Zhao, Q., Neshat, S., Heinrichs, D.E. and Bianco, N. (1996) Expression of the multidrug resistance operon *mexA-mexB-oprM* in *Pseudomonas aeruginosa*: *mexR* encodes a regulator of operon expression. Antimicrob. Agents Chemother. 40, 2021–2028.

[9] Ziha-Zarifi, I., Llanes, C., Kohler, T., Pechere, J.C. and Plesiat, P. (1999) In vivo emergence of multidrug-resistant mutants of *Pseudomonas aeruginosa* overexpressing the active efflux system MexA-MexB-OprM. Antimicrob. Agents Chemother. 43, 287–291.

[10] Yoneyama, H., Ocaktan, A., Tsuda, M. and Nakae, T. (1997) The role of *mex*-gene products in antibiotic extrusion in *Pseudomonas aeruginosa*. Biochem. Biophys. Res. Commun. 233, 611–618.

[11] Sambrook, J., Fritsch, E.F. and Maniatis, T. (1989) Molecular Cloning: A Laboratory Manual, 2nd edn. Cold Spring Harbor Laboratory Press, Cold Spring Harbor, NY.

[12] Schafer, A., Tauch, A., Jager, W., Kalinowski, J., Thierbach, G. and Puhler, A. (1994) Small mobilizable multi-purpose cloning vectors derived from the *Escherichia coli* plasmids pK18 and pK19: selection of defined deletions in the chromosome of *Corynebacterium glutamicum*. Gene 145, 69–73.

[13] Parales, R.E. and Harwood, C.S. (1993) Construction and use of a new broad-host-range *lacZ* transcriptional fusion vector, pHRP309, for gram$^-$ bacteria. Gene 133, 23–30.

[14] Evans, K. and Poole, K. (1999) The MexA-MexB-OprM multidrug efflux system of *Pseudomonas aeruginosa* is growth-phase regulated. FEMS Microbiol. Lett. 173, 35–39.

Biochemical and Biophysical Research Communications **261**, 452–455 (1999)
Article ID bbrc.1999.1045, available online at http://www.idealibrary.com on IDEAL®

Interplay between the Efflux Pump and the Outer Membrane Permeability Barrier in Fluorescent Dye Accumulation in *Pseudomonas aeruginosa*

Monika Germ, Eisaku Yoshihara, Hiroshi Yoneyama, and Taiji Nakae
Department of Molecular Life Science, School of Medicine, Tokai University, Isehara 259-1193, Japan

Received April 20, 1999

Pseudomonas aeruginosa **encodes three types of xenobiotic efflux pumps, MexAB-OprM, MexCD-OprJ, and MexEF-OprN, which are regulated by the *nalB*, *nfxB*, and *nfxC* genes, respectively, and their high expression renders the cells resistant to multiple species of antibiotics. We evaluated the role of the outer membrane permeability barrier and the efflux pump in lowering the intracellular concentration of fluorescent probes. The wild-type, *nalB*, *nfxB*, and *nfxC* strains with an intact outer membrane showed equally high capability in draining out intracellular fluorescent dye, 2-(4-dimethylaminostyryl)-1-ethylpyridinium and ethidium bromide. When the outer membrane barrier was dismantled by the EDTA treatment, wild-type, *nfxC*, *nfxB*, and *nalB* strains showed significantly different levels of dye accumulation. The polymyxin B-treated cells showed an even more pronounced difference in dye accumulation among the *nfxC*, *nfxB*, and *nalB* mutants. We concluded from these results that the xenobiotic extrusion pumps interplay with the outer membrane permeability barrier in lowering the intracellular substrate concentration. Among three extrusion pumps in *P. aeruginosa*, MexAB-OprM was the most efficient, followed by MexCD-OprJ and MexEF-OprN pumps for the fluorescent dye extrusion.** © 1999 Academic Press

Low specific antibiotic resistance in gram-negative bacteria is mainly attributable to a tight diffusion barrier at the outer membrane and active drug extrusion (1, 2). Natural resistance of bacteria to structurally and functionally different antibiotics could be responsible for serious set-backs during antimicrobial chemotherapy (3–7). In addition, high selective pressure exerted by world-wide uncontrolled use of antibiotics changes the situation even worse rapidly. *P. aeruginosa* is a problematic pathogen in immunocompromised patients due mainly to its high and broad resistance to antibiotics (7). Multidrug resistance in *P. aeruginosa* is mainly attributable to the expression of three multidrug extrusion systems, namely, MexAB-OprM (8–10), MexCD-OprJ (11) and MexEF-OprN (12). Among these, only the MexAB-OprM pump is expressed in the wild-type strain and the MexAB-OprM, MexCD-OprJ and MexEF-OprN pumps are overexpressed upon mutation of the respective regulatory genes (13–15).

The substrate specificities of these efflux pumps appeared similar and could only be distinguished by measuring the antimicrobial susceptibility profile of the mutant strains (16). Therefore, biochemical methods to quantitate their xenobiotics extrusion capability and to differentiate these efflux pumps have been long-awaited. We have reported recently that the MexAB-OprM machinery recognizes several fluorescent dyes as the substrate and exports them efficiently (17). Expanding this real-time fluorescence measurement method in combination with the outer membrane permeabilizing agents, we characterized the interplay between the outer membrane permeability barrier and the efflux pump.

MATERIALS AND METHODS

Reagents and antibiotics. Reagents were purchased from the following sources and used without further purification. 2-(4-dimethylaminostyryl)-1-ethylpyridinium (DMP) and polymyxin B were from Sigma Chemical Co (St. Louis, MA). Ethidium bromide was from Dojindo Laboratories (Japan). Ethylene-diaminetetraacetic acid (EDTA) was from Wako Chemicals (Japan).

Bacterial strains and growth conditions. Strains used in this study are listed in Table 1. All the strains were grown at 37°C in LB medium (1% of tryptone, 0.5% of yeast extract, 0.5% of NaCl, pH 7.2 per liter). Experimental cultures inoculated at 5% with a fully grown overnight culture were rotated at 200 rpm at 37°C for 2 h. The *nalB*-type mutant was isolated from laboratory strain, PAO4290, by the procedure described earlier (18).

Preparation of cell suspension and fluorescence measurements. Cells were harvested at 7000 × g for 10 min at 25°C, washed once with 100 mM NaCl-50 mM sodium phosphate buffer (pH 7.8), and suspended again in the same buffer at $A_{600nm}^{1cm} = 0.1$ (final concentration) in the presence of 0.05% of glycerol. Cells were used within 2 h after cell preparation. Fluorescence measurements were carried out at pH 7.0 under controlled temperature at 30°C. DMP was dissolved in absolute methanol and ethidium bromide in water and added to

0006-291X/99 $30.00

TABLE I
Bacterial Strains

Strains	Relevant properties	Reference
Pseudomonas aeruginosa		
PAO4290	*leu-10, argF10, aph-9004, FP*$^-$	Matsumoto collection
TNP30	*nalB* derivative of PAO4290	This laboratory
8380OR01	*nfxB* derivative of 8380	16
8380OIR01	*nfxC* derivative of 8380	16

the final concentrations as indicated in the figure legends. Fluorescence intensity was measured with a Hitachi 650-10S Fluorescence-Spectrophotometer and the data were registered on a Hitachi 056 recorder. Excitation and emission wavelengths for DMP were, respectively, 485 and 577 nm, and for ethidium bromide, 520 and 590 nm. Slit widths were set at 5 nm for excitation and at 10 nm for emission for all measurements.

RESULTS

We reported recently that the fluorescent dye DMP could be used as a substrate for real-time monitoring of the MexAB-OprM efflux pump function (17). When the DMP accumulation was determined in the wild-type and the *nalB, nfxB* and *nfxC* strains, all the cells accumulated an undetectable level of fluorescent dye indicating that all the efflux machineries pumped out the dye efficiently (Fig. 1A). Our previous study reported that the mutant expressing none of these pumps accumulated a large amount of dye (17). Therefore, the presence of the efflux pump is essential in lowering the intracellular DMP concentration. We interpreted the above observation to mean that the outer membrane barrier masks the different dye extrusion capability in these strains, since it was assumed that the outer membrane barrier and the efflux pumps are linked in efficient lowering of the intracellular dye concentration.

Effect of EDTA treatment on DMP accumulation. We treated the cells with 0.1 mM EDTA to dismantle the outer membrane barrier and measured the DMP accumulation. When 50 μM DMP was added to the suspension of EDTA-treated cells, the wild-type strain accumulated a significantly high amount of DMP with an increment rate of 26 arbitrary units. The rate in the *nfxC nfxB* and *nalB* mutants was 10, 6 and 0 units, respectively (Fig. 1B). We interpreted this result to mean that the level of the MexAB-OprM extrusion pump expressed in the wild-type cell is insufficient to drain out incoming DMP through the damaged outer membrane. On the other hand, the *nalB*-type mutant accumulated an undetectable level of DMP, even in the presence of EDTA suggesting that the MexAB-OprM pump in the *nalB* mutant reserves enough potential to drain out all incoming DMP rapidly. The MexEF-OprN as well as the MexCD-OprJ pump systems did not appear to drain off the massive level of incoming dye in the EDTA-treated cells, but still reserve a certain capacity to extrude the dye more efficiently than the wild-type strains.

Effect of polymyxin B treatment on DMP accumulation. We described above that the use of the fluorescent dyes allowed us to distinguish the *nalB* strains from the *nfxC* or *nfxB* strain in terms of dye extrusion capability, but the *nfxC* and *nfxB* strains were similar in this respect (Fig. 1B). We used another membrane permeabilizing agent, polymyxin B that permeabilizes the outer mem-

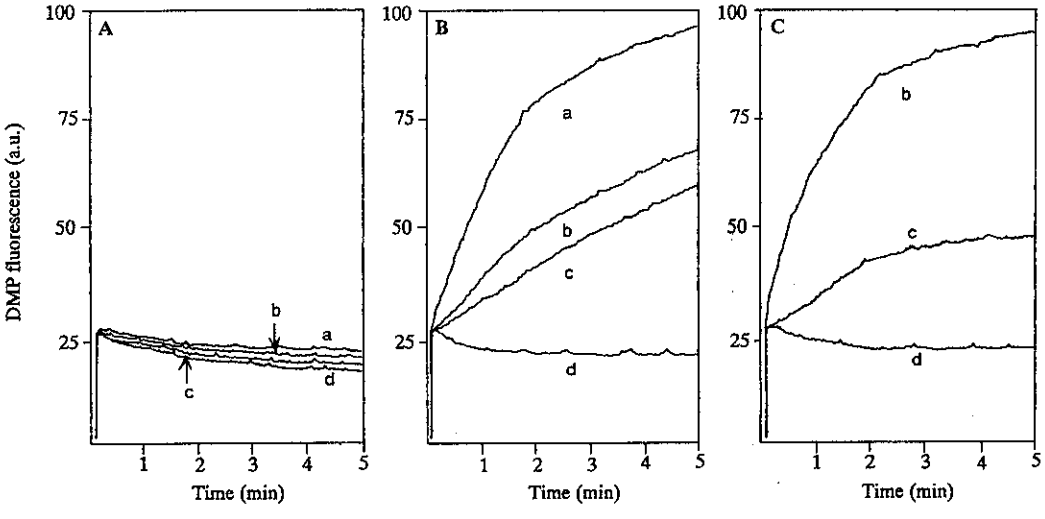

FIG. 1. Effect of EDTA and polymyxin B in the efflux pump-mediated lowering of intracellular DMP. Cells were treated with 0.1 mM EDTA or 2.5 μg/ml of polymyxin B and kept at 30°C for 5 min, and then 50 μM DMP in absolute methanol was added. The fluorescent intensity was recorded immediately. (A) Without pretreatment. (B) EDTA treatment. (C) Polymyxin B treatment. Strains: (a) PAO4290; (b) 8380OIR01; (c) 8380OR01 (d) TNP30.

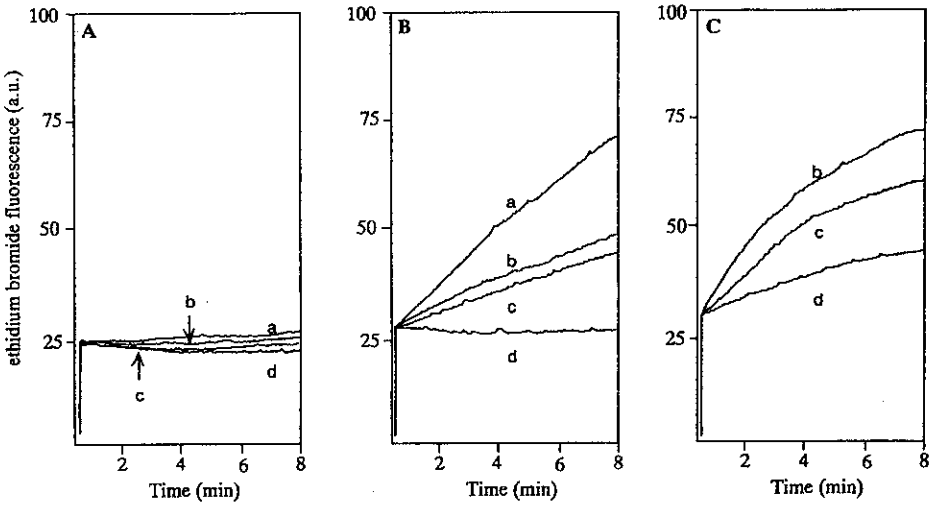

FIG. 2. Effect of EDTA and polymyxin B in the efflux pump-mediated lowering of intracellular ethidium bromide. Cells were treated with 0.1 mM EDTA or 2.5 μg/ml of polymyxin B and kept at 30°C for 5 min, and then 10 μM ethidium bromide in water was added. The fluorescent intensity was recorded immediately. (A) Without pretreatment. (B) EDTA treatment. (C) Polymyxin B treatment. Strains: (a) PAO4290; (b) 8380OIR01; (c) 8380OR01 (d) TNP30.

brane to hydrophobic agents (19). We treated the cells with 2.5 μg/ml of polymyxin B and measured the DMP accumulation. The *nfxB* strains showed an increment rate of 6.6 arbitrary units, which was significantly lower than the rate of 32.4 units in the *nfxC* strain. The *nalB* strain again showed nearly undetectable fluorescence increments under the same conditions (Fig. 1C). We interpreted these results to mean that polymyxin B dismantled the outer membrane permeability barrier more efficiently than EDTA, thereby allowing a very rapid influx of the dye, in which the MexCD-OprJ pump still retained a certain capability to drain out the incoming DMP, although the capability of the MexEF-OprN pump was saturated.

Effect of EDTA and Polymyxin B treatment on ethidium bromide accumulation. In contrast to DMP, which mainly monitors accumulation of the dye to the cytoplasmic membrane, ethidium bromide uptake reflects the dye accumulation into the cytoplasmic compartment (16). We found that the *nalB, nfxC* and *nfxB* cells can recognize ethidium bromide as a substrate and extrude efficiently resulting in a nearly undetectable level of the accumulated dye in intact cells (Fig. 2A). Again the mutant lacking MexAB-OprM accumulated a large amount of ethidium bromide suggesting that the efflux pump actively lowered the intracellular dye concentration (17). When the EDTA-treated cells were subjected to the ethidium bromide accumulation experiment, the increment rate in the *nfxB* and *nfxC* mutants were 3.6 and 4.9 units, respectively (Fig. 2B). The results were consistent with the DMP accumulation experiments in the presence of EDTA. Again, the *nalB* mutant showed no significant increase in dye accumulation under the same conditions (Fig. 2B). Experiments with the polymyxin B-treated cells showed more pronounced differences between the mutants (Fig. 2C). The increment rate in the *nfxC* strains was 16 units, followed by the *nfxB* strain with 9.4 units. Thus, it became clear that among the multidrug resistant strains of *P. aeruginosa,* the MexAB-OprM pump retains the highest capability in lowering the intracellular ethidium bromide concentration followed by the MexCD-OprJ and MexEF-OprN pump assemblies. The clinical isolates of *nalB, nfxB* and *nfxC* mutants were subjected to the dye extrusion experiments and appeared to behave as the respective laboratory mutants (data not shown).

DISCUSSION

We reported in this study that *nalB, nfxC, nfxB* and the wild-type cells with an intact outer membrane efficiently lowered the intracellular dye concentration to an undetectable level. Treatment of the cells with EDTA or polymyxin B to dismantle the outer membrane barrier resulted in a high level of dye accumulation in the wild-type cells. The wild-type level of the extrusion capability, which is most likely due to low expression of the MexAB-OprM extrusion pump, was not strong enough to overcome massive influx of the dye. On the other hand, the *nalB* cells still reserved enough potential to drain out all incoming dyes through the damaged outer membrane. The dye extrusion capability of the *nfxB* and *nfxC* cells was saturated partially and appeared to be intermediate between the *nalB* and the wild-type strain. The polymyxin B-treated *nfxC* cells accumulated more dye than the *nfxB* cells. Therefore, the dye exporting capability among these strains was the highest in the *nalB* mutant, followed by the *nfxB* and *nfxC* mutants and the wild type

strain. An alternative interpretation of the high dye accumulation in the EDTA- or polymyxin B-treated cells would be that these agents damaged the subunit interaction of the extrusion machinery. However, this was not the case, since the EDTA-treated wild-type strain accumulated a significantly lower level of the dyes than the mutant lacking the MexAB-OprM pump. Therefore, we concluded that a high level of dye accumulation in the EDTA or polymyxin B-treated cells is attributable to the increased outer membrane permeability.

The role of outer membrane permeability in tetracycline accumulation in *Escherichia coli* was reported earlier with emphasis on the importance of the porin channel as the diffusion pathway (2). However, the situation in *P. aeruginosa* is largely different from that of *E. coli*. Since the porin channel in *P. aeruginosa* is too small to allow the passage of most antibiotics and the fluorescent dyes (20). Therefore, the role of the outer membrane barrier in the interplay with the efflux pump in *P. aeruginosa* has to be emphasized. The efficacy of substrate extrusion reflects the affinity of the efflux pump to the substrate and the level of the pump expression. In fact the accumulation of 1-(4-trimethylammoniumphenyl)-6-phenyl-1,3,5-hexatriene was higher in the *nalB* mutant than in the *nfxC* and *nfxB* mutants (data not shown). Therefore, precise transport K_m and V_{max} should be calculated with an improved experimental set up in the future.

In summary, this study reported on the different capacity of the efflux pumps of *P. aeruginosa* in fluorescent dye extrusion. The dye extrusion efficiency of the *nalB*, *nfxB* and *nfxC* reported here was also confirmed using an independent series of the same mutants. This is the first report that enabled us to distinguish the *nalB*, *nfxB* and *nfxC* mutants by real-time measurements of the substrate accumulation.

ACKNOWLEDGMENTS

This study was financially supported in part by the following grants: The Japan Society for the Promotion of Science, The Ministry of Education, Science, Sports and Culture of Japan, The Ministry of Health and Welfare of Japan, and Tokai University School of Medicine, research project.

REFERENCES

1. Nikaido, H. (1994) *Science* **264,** 382–388.
2. Thanassi, D. G., Suh, G. S., and Nikaido, H. (1995) *J. Bacteriol.* **177,** 998–1008.
3. Aubert, G., Pozetto, B., and Dorche, G. (1992) *J. Antimicrob. Chemother.* **29,** 307–312.
4. Paulsen, I. T., Brown, M. H., and Skurray, R. A. (1996) *Microbiol. Rev.* **60,** 575–608.
5. Nikaido, H. (1996) *J. Bacteriol.* **178,** 5853–5859.
6. George, M. A. (1996) *FEMS Microbiol. Lett.* **139,** 1–10.
7. Nakae, T., Yoshihara, E., and Yoneyama, H. (1997) *J. Infect Chemother.* **3,** 173–183.
8. Poole, K., Krebes, K., McNally, C., and Neshat, S. (1993) *J. Bacteriol.* **175,** 7363–7372.
9. Li, X.-Z., Nikaido, H., and Poole, K. (1995) *Antimicrob. Agents Chemother.* **39,** 1948–1953.
10. Morshed, S. R., Lei, Y., Yoneyama, H., and Nakae, T. (1995) *Biochem. Biophys. Res. Commun.* **210,** 356–362.
11. Poole, K., Gotoh, N., Tsujimoto, H., Zhao, Q., Wada, A., Yamasaki, T., Neshet, S., Yamagishi, J.-I., Li, X.-Z., and Nishino, T. (1996) *Mol. Microbiol.* **21,** 713–724.
12. Köhler, T., Michéa-Hamzehpour, M., Henze, U., Gotoh, N., Curty, L. K., and Péchère, J.-C. (1997) *Mol. Microbiol.* **23,** 345–354.
13. Rella, M., and Haas, D. (1982) *Antimicrob. Agents Chemother.* **22,** 242–249.
14. Hirai, K., Suzue, S., Irikura, T., Iyobe, S., and Mitsuhashi, S. (1987) *Antimicrob. Agents Chemother.* **31,** 582–586.
15. Fukuda, H., Hosaka, M., Hirai, K., and Iyobe, S. (1990) *Antimicrob. Agents Chemother.* **34,** 1757–1761.
16. Masuda, N., Sakagawa, E., and Ohya, S. (1995) *Antimicrob. Agents Chemother.* **39,** 645–649.
17. Ocaktan, A., Yoneyama, H., and Nakae, T. (1997) *J. Biol. Chem.* **272,** 21964–21969.
18. Lei, Y., Sato, K., and Nakae, T. (1991) *Biochem. Biophys. Res. Commun.* **178,** 1043–1048.
19. Vaara, M. (1992) *Microbiol. Rev.* **56,** 395–411.
20. Nakae, T. (1995) *Microbiol. Immunol.* **39,** 221–229.

ANTIMICROBIAL AGENTS AND CHEMOTHERAPY, May 1999, p. 1301–1303 Vol. 43, No. 5
0066-4804/99/$04.00+0

Resistance to β-Lactam Antibiotics in *Pseudomonas aeruginosa* Due to Interplay between the MexAB-OprM Efflux Pump and β-Lactamase

TAIJI NAKAE,* AKIRA NAKAJIMA, TOSHIHISA ONO, KOHJIRO SAITO, AND HIROSHI YONEYAMA

Department of Molecular Life Science, Tokai University School of Medicine, Isehara 259-1193, Japan

Received 7 December 1998/Returned for modification 8 February 1999/Accepted 3 March 1999

We evaluated the roles of the MexAB-OprM efflux pump and β-lactamase in β-lactam resistance in *Pseudomonas aeruginosa* by constructing OprM-deficient, OprM basal level, and OprM fully expressed mutants from β-lactamase-negative, -inducible, and -overexpressed strains. We conclude that, with the notable exception of imipenem, the MexAB-OprM pump contributes significantly to β-lactam resistance in both β-lactamase-negative and β-lactamase-inducible strains, while the contribution of the MexAB-OprM efflux system is negligible in strains with overexpressed β-lactamase. Overexpression of the efflux pump alone contributes to the high level of β-lactam resistance in the absence of β-lactamase.

A major problem in *Pseudomonas aeruginosa* infection is that this organism exhibits natural and acquired resistance to many structurally and functionally diverse antibiotics. The multiple antibiotic resistance of this organism is mainly caused by low outer membrane permeability (11) and the expression of efflux pumps. Three efflux pumps have been documented (4, 5, 8, 14, 15) so far, namely the MexAB-OprM (10, 13), the MexCD-OprJ (12), and the MexEF-OprN (6) pumps. In the wild-type strain only the MexAB-OprM pump is expressed and the others are silent (4, 5, 10, 13). The *nalB* mutant overexpresses the MexAB-OprM pump (10, 13), rendering the bacterium more resistant than the wild-type strain to certain antibiotics (15). *P. aeruginosa* also expresses a chromosomally encoded β-lactamase in the presence of an appropriate inducer and shows elevated resistance to β-lactam antibiotics (2, 3). An earlier study predicted a possible interplay between membrane permeability and β-lactamase in β-lactam resistance in *P. aeruginosa* (7). Thus, it is important to ask which factor contributes most to resistance under various conditions. We addressed this issue by constructing a series of mutants producing different levels of the MexAB-OprM efflux pump and of β-lactamase.

Table 1 lists the strains used, their relevant properties, and β-lactamase activities. The strains PAO1, PAO4096, and TNP001 produce inducible, undetectable, and fully expressed β-lactamase, respectively (2, 17). We mutagenized the *oprM* gene by inserting a Tet^r cassette as reported earlier (18). Manipulation of DNA has been described earlier (16). We confirmed the Tet^r marker insertion by amplification of the chromosomal *oprM* by PCR as described by Ausubel et al. (1) by using the primers 5′-CAGTTGCAGCTGACCAAGG and 5′-TCGCTGGCCTTGACCAGATCG (data not shown). We confirmed by the Western blotting method with an anti-OprM antibody (18) that the mutants carrying the Tet^r insertion in *oprM* showed no detectable OprM protein (data not shown).

We evaluated the role of the efflux pump without β-lactamase by constructing OprM-deficient (ΔOprM), OprM-constitutive (OprM$^+$), and OprM-overexpressed (OprM^{+++}) mutants from a β-lactamase-negative strain (Bla$^-$) which produces less than 0.9×10^{-3} U of β-lactamase (Table 1). The β-lactam

TABLE 1. Bacterial strains, relevant properties, and β-lactamase activities[a]

Strain	Parent	Relevant property	β-Lactamase activity (U)		Reference or study
			Uninduced	Induced[b]	
PAO1		Wild type	2.7×10^{-3}	0.65	15
TNP024	PAO1	*nalB*-type derivative	2.8×10^{-3}	0.67	This study
TNP025	PAO1	Δ*oprM* (Tet^r insertion)	2.6×10^{-3}	0.59	This study
PAO4096	PAO4069	*blaP9206 BlaI9407 met9020 pro9024*	0.8×10^{-3}	0.9×10^{-3}	2
TNP026	PAO4096	*nalB*-type derivative	0.7×10^{-3}	ND[c]	This study
TNP027	PAO4096	Δ*oprM* (Tet^r insertion)	0.5×10^{-3}	0.6×10^{-3}	This study
TNP001	PAO1	β-lactamase fully expressed	2.55	2.03	17
TNP028	TNP001	*nalB*-type derivative	2.33	2.32	This study
TNP029	TNP001	Δ*oprM* (Tet^r insertion)	2.40	2.82	This study

[a] The *nalB*-type mutants were isolated as previously reported (8). The β-lactamase assay used was also previously reported (17). One unit of β-lactamase hydrolyges 1 μmol of cephalothin per min per mg of protein.
[b] β-Lactamase was induced in the presence of 0.15 μg of imipenem/ml.
[c] ND, not detected.

* Corresponding author. Mailing address: Department of Molecular Life Science, Tokai University School of Medicine, Isehara 259-1193, Japan. Phone: 81-465-93-5436. Fax: 81-463-93-5437. E-mail: nakae@is.icc.u-tokai.ac.jp.

TABLE 2. MICs of antibiotics for strains with different levels of OprM expression and β-lactamase production[a]

Strain	MIC (μg/ml)										
	CAZ	CZOP	CFPM	CPR	CBPC	AZT	IPM	MPM	CPZ	CP	OFLX
PAO1	0.78	0.78	0.78	1.56	25	3.13	0.78	0.39	3.13	25	0.39
TNP024	3.13	1.56	3.13	3.13	100	12.5	0.78	0.78	12.5	200	1.56
TNP025	0.39	0.2	0.1	0.2	0.39	0.2	0.78	0.1	0.39	1.56	0.05
PAO4096	0.78	0.2	0.39	0.78	12.5	1.56	0.2	0.2	0.78	25	0.2
TNP026	3.13	0.78	1.56	3.13	50	12.5	0.2	0.78	6.25	200	1.56
TNP027	0.39	0.1	0.1	0.1	0.2	0.2	0.2	<0.013	0.2	1.56	0.05
TNP001	50	50	25	50	200	50	0.78	1.56	400	50	0.39
TNP028	50	50	25	50	400	50	0.78	3.13	400	>200	1.56
TNP029	50	25	12.5	50	100	25	0.78	0.78	400	1.56	0.05

[a] MICs were determined by the agar dilution method with Mueller-Hinton agar (Becton-Dickinson). Abbreviations: CAZ, ceftazidime; CZOP, cefozopran; CFPM, cefepime; CPR, cefpirome; CBPC, carbenicillin; AZT, aztreonam; IPM, imipenem; MPM, meropenem; CPZ, cefoperazone; CP, chloramphenicol; OFLX, ofloxacin.

MICs for the Bla$^-$ OprM^{+++} derivative (TNP026) were 8 to 250 times higher than those for the Bla$^-$ ΔOprM strain (TNP027). These increases in MICs are attributable to the *nalB* mutation, notably overexpression of the MexAB-OprM pump. This new finding clearly shows that overexpression of the efflux pump alone confers high β-lactam resistance without β-lactamase. The β-lactam MICs for the Bla$^-$ OprM$^+$ strain (PAO4096) were 2 to 64 times higher than those for the Bla$^-$ ΔOprM mutant (TNP027) except for meropenem. The higher MICs for PAO4096 than for TNP027 reflect the fraction that the basal level of the MexAB-OprM efflux pump contributes to the intrinsic β-lactam resistance. This result is consistent with recently reported conclusions (9).

Experiments using the strains with fully expressed β-lactamase (Bla^c OprM$^+$, TNP001), an ΔOprM derivative (TNP029), and an OprM^{+++} derivative (TNP028) showed entirely different MIC profiles. First of all, the β-lactam MICs for the Bla^c ΔOprM strain (TNP029) were 64 to 2,000 times higher than those for the Bla$^-$ ΔOprM mutant (TNP027). This large difference in MICs appears to be due solely to the contribution of the fully expressed β-lactamase (Table 2). The contributions of wild-type and elevated levels of MexAB-OprM expression in the TNP001 strain to the MICs of these β-lactams were nearly masked by high β-lactamase production, since the MICs of these antibiotics for the OprM^{+++} derivative, TNP028, were only one to four times higher than those for TNP029. Based on these new findings, we conclude that in the β-lactamase fully expressed strain, the β-lactamase predominates in causing β-lactam resistance and the role of the efflux pump is secondary.

In the next experiment, we designed an experiment taking a wild-type laboratory strain (PAO1) and constructing ΔOprM (TNP025) and *nalB* (TNP024) mutants. The β-lactamase activities of these strains in the presence and absence of the inducer were 0.59 to 0.67 U and 2.6×10^{-3} to 2.8×10^{-3} U, respectively (Table 1). The β-lactam MICs for the wild-type strain, PAO1, were 0.39 to 25 μg/ml, and these values were unexpectedly only one to four times higher than the MICs of these antibiotics for the Bla$^-$ counterpart (PAO4096). These results clearly indicate that the contribution of β-lactamase to the MICs of these β-lactams was marginal. This is probably due to poor β-lactamase inducibility of the β-lactams used, since the MICs of these antibiotics for the Bla^c strain (TNP001) were very high (Table 2).

To determine the role of the efflux pump in β-lactam resistance, we compared the MICs of antibiotics for the Bla^i OprM$^+$ (PAO1) and the Bla^i ΔOprM (TNP025) strains. The β-lactams MICs for PAO1 were 2 to 64 times higher than those for TNP025, indicating that the low-level expression of the efflux pump mainly contributes to the intrinsic resistance. This result is consistent with that of a recent report (9). In addition, the MICs of these antibiotics for the Bla^i OprM^{+++} strain were 8- to 256-fold higher than those for the Bla^i ΔOprM strain (TNP025). These results showed that the efflux pump alone can confer very high β-lactam resistance with a negligible contribution of β-lactamase. To ascertain the contribution of inducible β-lactamase to β-lactam resistance in the MexAB-OprM-overexpressed environment, we compared the MICs of β-lactams for TNP024 and TNP026 and found that the MICs for TNP024 were only one to two times higher than those for TNP026, indicating again that the contribution of inducible β-lactamase was small compared with that of the efflux pump under these conditions. After this paper was submitted for publication, Masuda et al. reported on the interplay between β-lactamase and the efflux pump (9). Our results concur in part with theirs and add additional results.

This study was supported by grants from the Ministry of Education, the Ministry of Health and Welfare, the Japan Society of Promotion of Science, and the Tokai University School of Medicine.

REFERENCES

1. **Ausubel, F. M., R. Brent, R. E. Kingston, D. D. Moore, J. G. Seidman, J. A. Smith, and K. Struhl.** 1995. Current protocols in molecular biology. Greene and Wiley Interscience, New York, N.Y.
2. **Bryan, L. E., S. Kwan, and J. A. Godfrey.** 1984. Resistance of *Pseudomonas aeruginosa* mutants with altered control of chromosomal β-lactamase to piperacillin, ceftazidime, and cefsulodin. Antimicrob. Agents Chemother. **25**:382–384.
3. **Bryan, L. E.** 1979. Resistance to antimicrobial agents: the general nature of the problem and the basis of resistance, p. 219–270. *In* R. G. Dogget (ed.), *Pseudomonas aeruginosa*. Clinical manifestation of infection and current therapy. Academic Press, New York, N.Y.
4. **Fukuda, H., M. Hosaka, K. Hirai, and S. Iyobe.** 1990. New norfloxacin resistance gene in *Pseudomonas aeruginosa* PAO. Antimicrob. Agents Chemother. **34**:1757–1761.
5. **Hirai, K., S. Suzue, T. Irikura, S. Iyobe, and S. Mitsuhashi.** 1987. Mutations producing resistance to norfloxacin in *Pseudomonas aeruginosa*. Antimicrob. Agents Chemother. **31**:582–586.
6. **Köhler, T., M. Michéa-Hamzehpour, V. Henze, N. Gotoh, L. K. Curty, and J.-C. Pechére.** 1997. Characterization of MexE-MexF-OprN, a positively regulated multidrug efflux system of *Pseudomonas aeruginosa*. Mol. Microbiol. **23**:345–354.
7. **Livermore, D. M., and K. W. M. Davy.** 1991. Invalidity for *Pseudomonas aeruginosa* of an accepted model of bacterial permeability to β-lactam antibiotics. Antimicrob. Agents Chemother. **35**:916–921.
8. **Lei, Y., K. Sato, and T. Nakae.** 1991. Ofloxacin-resistant *Pseudomonas aeruginosa* mutants with elevated drug extrusion across the inner membrane. Biochem. Biophys. Res. Commun. **178**:1043–1048.
9. **Masuda, N., N. Gotoh, C. Ishii, E. Sakagawa, and T. Nishino.** 1999. Interplay between chromosomal β-lactamase and the MexAB-OprM efflux system in intrinsic resistance to β-lactams in *Pseudomonas aeruginosa*. Antimicrob. Agents Chemother. **43**:400–402.
10. **Morshed, S. R., Y. Lei, H. Yoneyama, and T. Nakae.** 1995. Expression of genes associated with antibiotic extrusion in *Pseudomonas aeruginosa*. Bio-

chem. Biophys. Res. Commun. **210**:356–362.
11. **Nikaido, H.** 1989. Outer membrane barrier as a mechanism of antimicrobial resistance. Antimicrob. Agents Chemother. **33**:1831–1836.
12. **Poole, K., N. Gotoh, H. Tsujimoto, Q. Zhao, A. Wada, T. Yamasaki, S. Neshat, J. Yamagishi, X.-Z. Li, and T. Nishino.** 1996. Overexpression of the *mexC-mexD-oprJ* efflux operon in *nfxB*-type multidrug resistant strain of *Pseudomonas aeruginosa*. Mol. Microbiol. **21**:713–724.
13. **Poole, K., K. Krebes, C. McNally, and S. Neshat.** 1993. Multiple antibiotic resistance in *Pseudomonas aeruginosa*: evidence for involvement of an efflux operon. J. Bacteriol. **175**:7363–7372.
14. **Poole, K., D. E. Heinrichs, and S. Neshat.** 1993. Cloning and sequence analysis of an EnvCD homologue in *Pseudomonas aeruginosa*: regulation by iron and possible involvement in the secretion of the siderophore pyoverdin. Mol. Microbiol. **10**:529–544.
15. **Rella, M., and D. Haas.** 1982. Resistance of *Pseudomonas aeruginosa* PAO to nalidixic acid and low levels of β-lactam antibiotics: mapping of chromosomal genes. Antimicrob. Agents Chemother. **22**:242–249.
16. **Sambrook, J., E. F. Fritsch, and T. Maniatis.** 1989. Molecular cloning: laboratory manual, 2nd ed. Cold Spring Harbor Laboratory Press, Cold Spring Harbor, N.Y.
17. **Satake, S., H. Yoneyama, and T. Nakae.** 1991. Role of OmpD2 and chromosomal β-lactamase in carbapenem resistance in clinical isolates of *Pseudomonas aeruginosa*. J. Antimicrob. Chemother. **28**:199–207.
18. **Yoneyama, H., A. Ocaktan, M. Tsuda, and T. Nakae.** 1997. The role of *mex* gene products in antibiotic extrusion in *Pseudomonas aeruginosa*. Biochem. Biophys. Res. Commun. **233**:611–618.

THE JOURNAL OF BIOLOGICAL CHEMISTRY
Vol. 274, No. 15, Issue of April 9, pp. 10517–10522, 1999
Printed in U.S.A.

Membrane Topology of the Xenobiotic-exporting Subunit, MexB, of the MexA,B-OprM Extrusion Pump in *Pseudomonas aeruginosa**

(Received for publication, October 26, 1998, and in revised form, January 6, 1999)

Lan Guan‡§, Michael Ehrmann‡¶‖, Hiroshi Yoneyama‡, and Taiji Nakae‡

From the ‡Department of Molecular Life Science, Tokai University School of Medicine, Isehara 259-1193, Japan and the ¶Department of Biology, University of Konstanz, Konstanz D-78457, Germany

The MexA,B-OprM efflux pump assembly of *Pseudomonas aeruginosa* consists of two inner membrane proteins and one outer membrane protein. The cytoplasmic membrane protein, MexB, appears to function as the xenobiotic-exporting subunit, whereas the MexA and OprM proteins are supposed to function as the membrane fusion protein and the outer membrane channel protein, respectively. Computer-aided hydropathy analyses of MexB predicted the presence of up to 17 potential transmembrane segments. To verify the prediction, we analyzed the membrane topology of MexB using the alkaline phosphatase gene fusion method. We obtained the following unique characteristics. MexB bears 12 membrane spanning segments leaving both the amino and carboxyl termini in the cytoplasmic side of the inner membrane. Both the first and fourth periplasmic loops had very long hydrophilic domains containing 311 and 314 amino acid residues, respectively. This fact suggests that these loops may interact with other pump subunits, such as the membrane fusion protein MexA and the outer membrane protein OprM. Alignment of the amino- and the carboxyl-terminal halves of MexB showed a 30% homology and transmembrane segments 1, 2, 3, 4, 5, and 6 could be overlaid with the segments 7, 8, 9, 10, 11, and 12, respectively. This result suggested that the MexB has a 2-fold repeat that strengthen the experimentally determined topology model. This paper reports the structure of the pump subunit, MexB, of the MexA,B-OprM efflux pump assembly. This is the first time to verify the topology of the resistant-nodulation-division efflux pump protein.

Nosocomial patients with cancer, transplantation, burn, cystic fibrosis, etc. are easily infected by bacteria with low virulence. Among those opportunistic pathogens, *Pseudomonas aeruginosa* is particularly problematic, since the bacteria show resistance to many structurally and functionally diverse antibiotics (1). Recent studies have revealed that this type of resistance is attributable to a synergy of low outer membrane permeability and active drug extrusion (2). An increasing number of multidrug extrusion systems are being reported in both prokaryotes and eukaryotes (2–8). It is likely, therefore, that active extrusion systems play a crucial role in the cellular defense mechanism against incoming noxious compounds in many living organisms. It is of great interest and importance, therefore, to analyze the mechanism by which such universally occurring extrusion pump function.

The wild-type *P. aeruginosa* expresses a low level of the MexA,B-OprM drug extrusion machinery (9, 10). Mutations in *nalB* gene cause overexpression of the *mexA,B-oprM* operon rendering the bacterium more resistant than the wild-type strain to a broad spectrum of antibiotics (3). Deletion of the coding region of the wild-type *mexA*, *mexB*, or *oprM* renders the mutant more susceptible than the wild-type strain to many antibiotics (9, 11). Thus, it is apparent that the MexA,B-OprM machinery is involved in the both basal and elevated levels of intrinsic antibiotic resistance in *P. aeruginosa*.

The MexA,B-OprM pump consists of three subunits, MexA, MexB, and OprM, located at the inner and outer membrane, respectively (9, 10). MexB consists of 1046 amino acid residues and is assumed to extrude the xenobiotics utilizing the proton motive force as the energy source (4, 12). This protein belongs to the resistant/nodulation/division (RND)[1] family (13, 14). MexA is an inner membrane-associated lipoprotein belonging to the membrane fusion protein family. OprM is an outer membrane protein probably forming the xenobiotics exit channel. A complex formation by these three subunit proteins has been suggested for many efflux pump assemblies in Gram-negative bacteria (13, 15–17). In fact, the functional coupling of the RND protein and the membrane fusion protein was recently demonstrated by the subunit exchange experiments using three efflux pump systems in *P. aeruginosa* (18–21), while the outer membrane components could be substituted with other proteins having a similar function. However, the precise molecular mechanism of substrate recognition and efflux through these pumps remained to be clarified. For a better understanding of how this pump extrudes the xenobiotics, it is essential to elucidate the structure and membrane topology of the individual pump subunit.

The membrane topology of several RND family proteins was suggested to have 12 transmembrane domains and two large hydrophilic domains (13, 22). Hydropathy analysis of MexB by the TOP-PRED II 1.1 software packages (23) suggested that it might have 12 certain and 5 putative transmembrane segments (TMS). Some other software predicted the presence of 11 TMS.

The topology of cytoplasmic membrane proteins in Gram-negative bacteria was often studied by the *phoA* gene fusion method. Alkaline phosphatase (AP) is enzymatically active after translocation to the periplasm, but is inactive when local-

* This work was supported by grants from the Ministry of Education of Japan, Science, Sports and Culture, the Ministry of Health and Welfare of Japan, the Japan Society for Promotion of Science, and the Tokai University School of Medicine Research Project. The costs of publication of this article were defrayed in part by the payment of page charges. This article must therefore be hereby marked "*advertisement*" in accordance with 18 U.S.C. Section 1734 solely to indicate this fact.

§ Recipient of the Tokai University School of Medicine Research Fellowship.

‖ Visited Tokai University with the support of the Japan Society for Human Science.

** To whom correspondence should be addressed. Tel.: 81-463-93-5436; Fax: 81-463-93-5437; E-mail: nakae@is.icc.u-tokai.ac.jp.

[1] The abbreviations used are: RND, resistance nodulation division; AP, alkaline phosphatase; TMS, transmembrane segment(s); PCR, polymerase chain reaction.

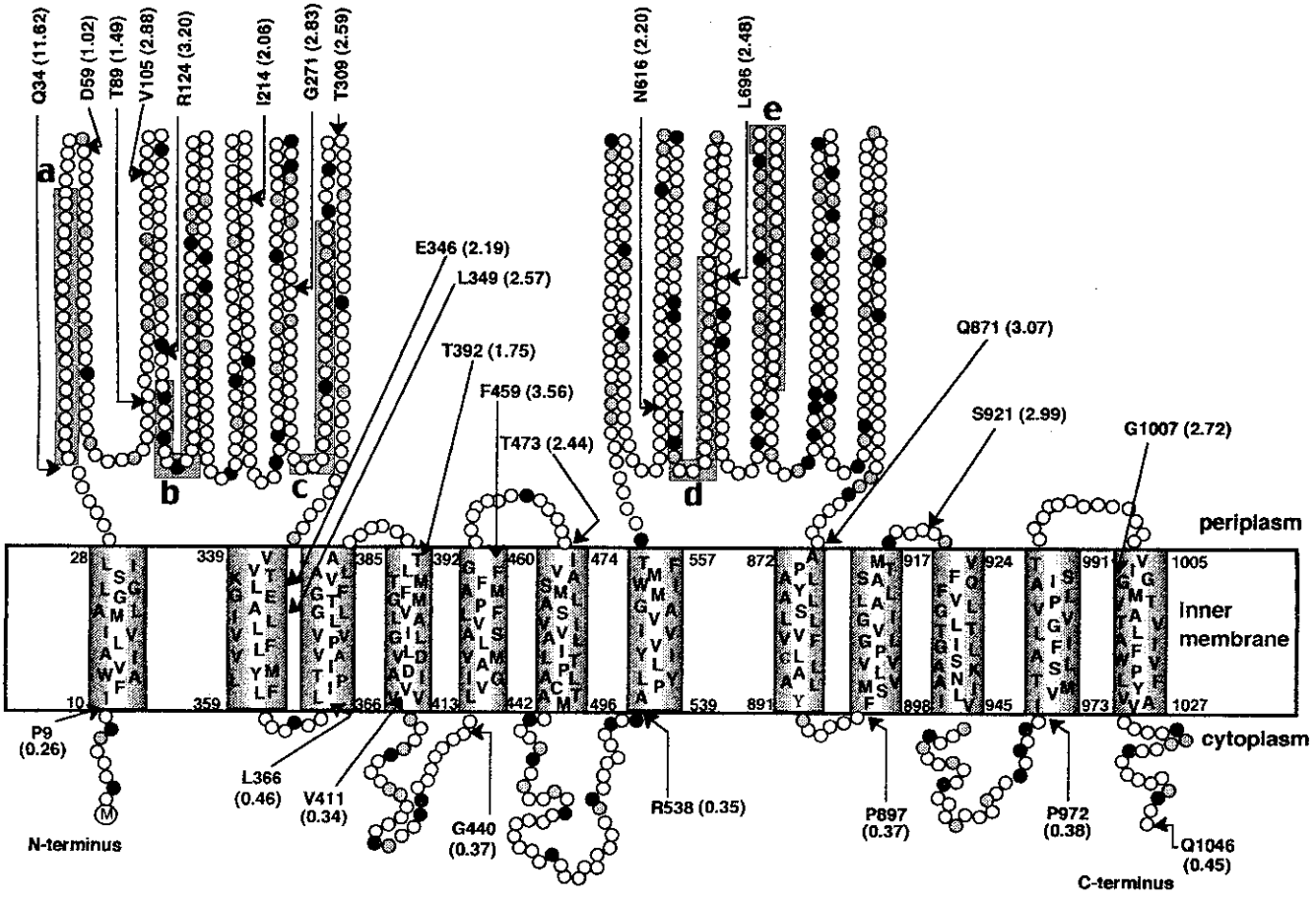

FIG. 1. **Schematic representation of the topological structure of the MexB protein.** Symbols: *filled circle*, positively charged amino acid; *shaded circle*, negatively charged amino acid; open circle, uncharged amino acid. Amino acid residues in transmembrane segments were expressed by a one-letter code. *Arrow*: one-letter code number in parentheses represents the fusion site-amino acid residue-AP activity (units). *Shaded rectangles around circles*, putative TMS. *a* through *e* are weak hydrophobic segments.

ized cytoplasmically (24, 25). Several tools, including Tn*phoA*, TnTAP, pPHO7, and pBAD*phoA* (24, 26, 27), have been developed to construct the *phoA* fusion to the target protein. Although transposon-mediated generation of gene fusion is simple, insertion of the reporter gene at a specific target site can be tedious. This difficulty is even more pronounced if a target protein has short extramembranous loops. An alternative method is cloning of PCR products to the 5′-end of the signal sequenceless *phoA* gene (28). Using these two methods, we analyzed the topology of MexB. This paper reports the two-dimensional transmembrane structure of MexB.

EXPERIMENTAL PROCEDURES

Bacteria and Plasmids—The *Escherichia coli* strains used were LMG194 [F⁻ Δ*ara714 leu*::Tn10 Δ*lacX74* Δ*phoA* (*Pvu*II) *galE galK thi rpsL*] (29) and CC118 (*araD139* Δ(*ara, leu*)7697 Δ*lacX*74 Δ*phoA*20 *galE galK thi rpsE rpoB argE*$_{am}$ *recA*1) (24). The plasmid pBAD*phoA* is a cloning vector containing a signal sequenceless *phoA* with a *Kpn*I cloning site just in front of *phoA*. The construction of pBAD*phoA* from pSWFII (30) and pBAD22 (29) will be described elsewhere. The transposon delivery plasmid pMM1 carries a mini-transposon TnTAP and Tn5 transposase (26). TnTAP contains a stretch of sequence coding for 24 amino acid residues, LTLIHKF*ENLYFQS*AAAMDPRVPC, including a tobacco etch virus protease cleavage site (underlined), signal sequenceless *phoA*, and *neo*. The Tn5 transposase is expressed *in trans*. The plasmid pMEXB1 was constructed by cloning a 3.9-kilobase *Sal*I fragment containing the wild-type *mexB* to the shuttle vector pMMB67EH (20).

Construction of mexB-phoA Fusions by PCR—Fusions of the truncated *mexB* to *phoA*, encoding for signal sequenceless AP, were carried out by inserting the PCR fragments of *mexB* into the 5′-end of the signal sequenceless *phoA* in pBAD*phoA*. Eleven out of 15 fusions were constructed by cloning the PCR fragments containing flanking *Kpn*I restriction sites into pBAD*phoA* cleaved with *Kpn*I. The PCR primer used for the 5′-end of the *mexB* gene was cccggtaccgTCGAAGTTTTTCATTGATAGG. The 3′-end primers designed for the immediately downstream of the codons Gln^{34}, Glu^{346}, Leu^{366}, Thr^{392}, Gly^{440}, Thr^{473}, Arg^{538}, Gln^{871}, Pro^{897}, Ser^{921}, and Cys^{972} were aggatggtacCTGGTTGACCGGCAGACTGAG (Gln^{34}), cgcgcggtacCTCGCCGAGGGTCTTCACTAC (Glu^{346}), gccgcggtacCAGCGTGGCGCGGAAG (Leu^{366}), cgcggtacCGTGTTGATCGAGAAGCC (Thr^{392}), ggcgcggtacCCCCTGGATCTGGCCCATGGA (Gly^{440}), cgcgcggtacCGTGATGGAGAACTGCCGGTAGAT (Thr^{473}), cgcggtacCCGATGCTTGAGGATCGAC (Arg^{538}), ccggcggtacCTGCGAGCCGGACAAGC (Gln^{871}), cgcggtacCGGAATCGACCAGCTTTCGTACAG (Pro^{897}), cccccggtacCGACAGGCCGCGCATGGACGTCG (Ser^{921}), and ccatcggtacCGGCCGCAGACGCAT (Pro^{972}), respectively. For the fusion of *phoA* to codons Gly^{1007} and Gln^{1046}, we designed the primers allowing in-frame blunt-end ligation, because there are two *Kpn*I sites in this part of *mexB*. The PCR fragments purified from agarose gel and blunted with the T4 DNA polymerase were ligated to the pBAD*phoA* cleaved by *Kpn*I and blunted with T4 DNA polymerase. The primer used for the 5′-end of the *mexB* gene was TCGAAGTTTTTCATTGATAGGCCC. Two 3′-end primers used to generate *phoA* fusions downstream of the codons Gly^{1007} and Gln^{1046} were cGCCGATCACGCCGGTACCGAT (Gly^{1007}) and aTTGCCCCTTTTCGACGGACGCCTGC (Gln^{1046}), respectively. For fusion pBAD-P9, two oligonucleotides containing the *Kpn*I sites at the both ends were annealed and ligated directly to the pBAD*phoA* cleaved with *Kpn*I. The oligonucleotides for coding and noncoding strands were CGTCGAAGTTTTTCATTGATAGGCCGGTAC and CGGCCTATCAATGAAAAACTTCGACGGTAC, respectively. The host cells used for analysis of AP activity was *E. coli* LMG194. For most fusion plasmids, codons for valine and proline residues were introduced at the 5′- and 3′-ends of the *mexB* fragments to introduce the *Kpn*I sites.

Construction of mexB-phoA Fusions by TnTAP—To obtain in-frame

TABLE I
Strain, plasmid, and the method for construction of the fusion

Strain	Fusion plasmid[a]	Method of construction
TNE040	pBADphoA	
TNE041	pBAD-P9	Olig[b]
TNE042	pBAD-Q34	PCR
TNE043	pBAD-E346	PCR
TNE044	pBAD-L366	PCR
TNE045	pBAD-T392	PCR
TNE046	pBAD-V411	PCR
TNE047	pBAD-G440	PCR
TNE048	pBAD-T473	PCR
TNE049	pBAD-R538	PCR
TNE050	pBAD-Q871	PCR
TNE051	pBAD-P897	PCR
TNE052	pBAD-S921	PCR
TNE053	pBAD-P972	PCR
TNE054	pBAD-G1007	PCR
TNE055	pBAD-Q1046	PCR
TNE056	pMEXB1	
TNE057	pMEXB-D59TAP	TnTAP
TNE058	pMEXB-T89TAP	TnTAP
TNE059	pMEXB-V105TAP	TnTAP
TNE060	pMEXB-R124TAP	TnTAP
TNE061	pMEXB-I214TAP	TnTAP
TNE062	pMEXB-G271TAP	TnTAP
TNE063	pMEXB-T309TAP	TnTAP
TNE064	pMEXB-L349TAP	TnTAP
TNE065	pMEXB-F459TAP	TnTAP
TNE066	pMEXB-N616TAP	TnTAP
TNE067	pMEXB-L696TAP	TnTAP

[a] AP was fused to the numbered amino acid residues.
[b] Oligonucleotide annealing method.

fusions of TnTAP to *mexB*, the pMM1 containing TnTAP was transformed into the strain *E. coli* CC118 carrying pMEXB1, which encodes the wild-type *mexB*. After transposition during overnight growth, a pool of plasmid DNA was isolated and digested with *Nhe*I to destroy pMM1, but not pMEXB1 and TnTAP. The restriction digests were transformed again into strain CC118. Blue colonies on agar plates containing 40 μg/ml 5-bromo-4-chloro-3-indolyl phosphate, 200 μg/ml ampicillin (for pMEXB1), and 100 μg/ml kanamycin were purified. Insertions into *mexB* were identified by PCR.

DNA Sequencing—The nucleotide sequence was determined using the ABI PRISM™ Dye Terminator Cycle Sequencing Core Kit with ampliTaq® DNA polymerase, FS. The sequencing primer used was GCAGTAATATCGCCCTGAGCAGC, reading out of the *phoA* gene toward the *mexB* gene. In addition, a primer GCGTCACACTTTGCTATGCC reading out of the pBAD*phoA* vector toward the *mexB* gene was also used.

Assay of AP Activity—AP activity was assayed by measuring the rate of hydrolysis of *p*-nitrophenyl phosphate in permeabilized cells as described elsewhere (31). One unit of AP activity corresponds to the rate of *p*-nitrophenyl phosphate hydrolysis, 1 μmol of *p*-nitrophenyl phosphate/min/mg of protein at 23 °C.

Expression of the Hybrid Proteins—For the Western blot analysis of the hybrid proteins, the crude envelope fraction and whole cell lysate were prepared as described elsewhere (10). SDS-polyacrylamide gel electrophoresis (10%) and Western blotting were carried out as described previously (32). The monoclonal antibody raised against AP was used to probe the hybrid proteins. Boiling the MexB protein in SDS caused disappearance of the protein band from the gel.

RESULTS

Construction of the mexB-phoA Fusions—To analyze the membrane topology of the MexB protein, we took the 12-TMS model for our working hypothesis and designed the experiments accordingly (Fig. 1). We constructed 25 clones expressing COOH-terminal-truncated MexB-AP hybrids and one clone (pBAD-Q1046) expressing *phoA* at the COOH-terminal end of full-length MexB using pBAD*phoA* and TnTAP (Table I). Cells harboring the pBAD-P9, pBAD-L366, pBAD-V411, pBAD-G440, pBAD-R538, pBAD-P897, pBAD-P972, and pBAD-Q1046 plasmids yielded pale blue colonies, suggesting that the AP domain is located in the cytoplasmic side of the inner membrane. The fusion pBAD-V411 was obtained accidentally in the course of pBAD-Q1046 construction. The remaining *mexB-phoA* fusions exhibited blue colonies on the 5-bromo-4-chloro-3-indolyl phosphate plates suggesting that the AP domain is translocated to the periplasm. The fusion joints were confirmed by nucleotide sequencing and all reading frames were correct (Tables II and III). The distribution of a total of 26 fusion sites covered the entire MexB protein, and each hydrophobic segment was flanked by *phoA* fusions (Fig. 1).

Alkaline Phosphatase Activities of the Cells Harboring the Fusion Plasmids—We quantified the AP activities of the cells harboring the *mexB-phoA* fusions (Fig. 1). The AP activities in

TABLE II
Nucleotide sequence of the mexB-phoA fusion junction derived from pBADphoA

The table shows the nucleotide sequence and the deduced amino acid sequence at the fusion junctions. Hyphens mark the fusion points. The DNA sequences of the *mexB* fragment amplified by PCR are indicated in bold. The lowercase letters represent the linker for the *Kpn*I restriction sites. Underlined sections represent the original bases of *mexB* and these alterations did not change the amino acid sequence. Small fonts show the inserted amino acid residues.

plasmid	Sequence of the *mexB-phoA* fusion junction	
	5′ end	3′ end
pBAD-P9	ATG gta c-cg **TCG AAG TTT** M V P S K F	**AGG CCG** ata c-CT GAC TCT C R P [1] P D S
pBAD-Q34	ATG gta c-cg **TCG AAG TTT** M V P S K F	**AAC CAG** gta c-CT GAC TCT N Q V P D S
pBAD-E346	ATG gta c-cg **TCG AAG TTT** M V P S K F	**GGC GAG** gta c-CT GAC TCT G E V P D S
pBAD-L366	ATG gta c-cg **TCG AAG TTT** M V P S K F	**ACG CTG** gta c-CT GAC TCT T L V P D S
pBAD-T392	ATG gta c-cg **TCG AAG TTT** M V P S K F	**AAC ACG** gta c-CT GAC TCT C N T V P D S
pBAD-V411	ATG - **TCG AAG TTT** M S K F	**GCC ATC GTC** G-CT GAC TCT A I V A D S
pBAD-G440	ATG gta c-cg **TCG AAG TTT** M V P S K F	**CAG GGG** gta c-CT GAC TCT C Q G V P D S
pBAD-T473	ATG gta c-cg **TCG AAG TTT** M V P S K F	**ATC ACG** gta c-CT GAC TCT C I T V P D S
pBAD-R538	ATG gta c-cg **TCG AAG TTT** M V P S K F	**CAT CGG** gta c-CT GAC TCT C H R V P D S
pBAD-Q871	ATG gta c-cg **TCG AAG TTT** M V P S K F	**TCG CAG** gta c-CT GAC TCT S Q V P D S
pBAD-P897	ATG gta c-cg **TCG AAG TTT** M V P S K F	**ATT CCG** gta c-CT GAC TCT I P V P D S
PBAD-S921	ATG gta c-cg **TCG AAG TTT** M V P S K F	**CTG TCG** gta c-CT GAC TCT C L S V P D S
pBAD-P972	ATG gta c-cg **TCG AAG TTT** M V P S K F	**CGG CCG** gta c-CT GAC TCT R P V P D S
pBAD-G1007	ATG - **TCG AAG TTT** M S K F	**ATC GGC** G -CT GAC TCT I G A D S
pBAD-Q1046	ATG - **TCG AAG TTT** M S K F	**GGG CAA** T-CT GAC TCT G Q S D S

[1] This isoleucine residue should be valine. This was accidentally replaced by an error in the oligonucleotide synthesis. However, this replacement did not affect the result.

these cells harboring the fusions derived from pBAD*phoA* were divided into two major classes. One class of cells showed about 0.2–0.4 unit of AP activity, which is close to the activity in the control cell (pBAD*phoA*, 0.32 unit) and another showed 1.7–11 units. Fusions at Pro^{9}, Leu^{366}, Val^{411}, Gly^{440}, Arg^{538}, Pro^{897}, Pro^{972}, and Gln^{1046} belonged to the former class. Therefore, these fusion sites are most likely to be located at the cytoplasmic side (Fig. 1). The remaining fusions, including the Gln^{34}, Glu^{346}, Thr^{392}, Thr^{473}, Gln^{871}, Ser^{921}, and Gly^{1007} sites, showed high AP activities, suggesting that these sites are located at the periplasmic side (Fig. 1).

All the cells harboring the *mexB-phoA* fusions derived from TnTAP showed an AP activity of about 1–3 units (Fig. 1), whereas the AP activity of cells containing *mexB* without *phoA* (pMEXB1) was only 0.33 unit. Based on these results, we concluded that all the fusion sites, including Asp^{59}, Thr^{89}, Val^{105}, Arg^{124}, Ile^{214}, Gly^{271}, Thr^{309}, Leu^{349}, Phe^{459}, Asn^{616}, and Leu^{696}, were located at the periplasmic side (Fig. 1).

Expression of the Hybrid Proteins—The expression of hybrid proteins derived from TnTAP and pBAD*phoA* is under the control of *lac* and *araBAD* promotor, respectively, and therefore the cells harboring the fusions were induced in the presence of 100 μM isopropyl-β-D-thiogalactopyranoside and 100 μM L-arabinose, respectively. The hybrid proteins with high and low AP activities are shown in Fig. 2, *lanes 3–20* and *lanes 21–27*, respectively. The size of the hybrid proteins was within the range of the expected molecular mass. The protein band of the fusion at Pro^{9} was undetectable, since the hybrid protein is expected to be soluble in the cytoplasm. All the bands for cytoplasmic hybrid proteins showed weaker signals than the periplasmic hybrid proteins, which probably was attributable to the proteolytic degradation of the hybrid protein as reported earlier (33, 34). In addition, protein bands with a higher molecular mass than expected were seen as reported elsewhere (35). This might be explained by suggesting that the chimeric proteins maintaining the native conformation bind less SDS than fully denatured proteins in the electrophoresis buffer, because the samples were subjected to electrophoresis without heating. Fusion Gly^{440} appeared only in a higher molecular weight range than expected and was barely seen.

TABLE III
Nucleotide sequence of the mexB-phoA fusion junction derived from TnTAP

The table shows the nucleotide sequence and the deduced amino acid sequence at the fusion junctions. Hyphens mark the fusion points. The DNA sequence from TnTAP is shown in bold.

plasmid	Sequence of the mexB-phoA fusion junction
pMEXB-D59TAP	ACG GTG CAG GAC – **CTG ACT CTT ATA** T V Q D L T L I
pMEXB-T89TAP	GGC AGC ATG ACC – **CTG ACT CTT ATA** G S M T L T L I
pMEXB-V105TAP	ATC GCC CAG GTC – **CTG ACT CTT ATA** I A Q V L T L I
pMEXB-R124TAP	GAA GTG CAG CGC – **CTG ACT CTT ATA** E V Q R L T L I
pMEXB-I214TAP	AAC GTG CAG ATT – **CTG ACT CTT ATA** N V Q I L T L I
pMEXB-G271TAP	GTA GGC CTG GGC – **CTG ACT CTT ATA** V G L G L T L I
pMEXB-T309TAP	ATC CGC CAG ACC – **CTG ACT CTT ATA** I R Q T L T L I
pMEXB-L349TAP	GAG GCG ATC CTC– **CTG ACT CTT ATA** E A I L L T L I
pMEXB-F459TAP	ATG GCG TTC TTC – **CTG ACT CTT ATA** M A F F L T L I
pMEXB-N616TAP	ACC GGC TTC AAC – **CTG ACT CTT ATA** T G F N L T L I
pMEXB-L696TAP	GAA GTC CTG CTC – **CTG ACT CTT ATA** E V L L L T L I

DISCUSSION

Most living organisms, if not all, seem to be equipped with xenobiotics extrusion pump(s). Mammalian cells, for instance, express P-glycoproteins (8), multidrug resistance associated protein (36), and cannalicular multispecific organic anion transporter (37), which extrude anticancer drugs, bile acids, and others. Expression of the efflux proteins in bacteria renders the organisms resistant to many antibiotics, organic solvents, hydrophobic dyes, and surfactants. Structure of the efflux pump in Gram-negative bacteria is particularly complicated, since the outer membrane covers the inner membrane. An extrusion pump in *P. aeruginosa* consisted of three subunits, MexA, MexB and OprM. Among them, MexB is particularly important in the pump function, since this subunit primarily recognizes and extrudes the substrates. To analyze the two-dimensional membrane topology of MexB, we constructed 26 *phoA* fusions, which covered the entire MexB protein.

The NH_2-terminal segment before the first hydrophobic segment consists of 9 amino acid residues containing 2 positively and 1 negatively charged residues. This segment is unlikely to cross the membrane according to the positive charge inside rule (38). The periplasmic location of the Gln^{34} and Gly^{1007} sites and the cytoplasmic location of the Pro^{9} and Gln^{1046} sites indicated that a cytoplasmic location of both the NH_2- and COOH-terminal ends (Fig. 1). The hybrid protein Gln^{34} was detected in the crude envelope fraction (Fig. 2, *lane 3*) indicating that TMS1 is an uncleaved signal-anchor. The periplasmic location of the Glu^{346}, Thr^{392}, Thr^{473}, Gln^{871}, Ser^{921}, and Gly^{1007} sites, and the cytoplasmic location of the Leu^{366}, Val^{411}, Gly^{440}, Arg^{538}, Pro^{897}, and Pro^{972} sites verified the transmembrane nature of the TMS 2–11 (Fig. 1). Five weak hydrophobic segments suggested by the TOPRED II software (*a–e*, Fig. 1) did not function as transmembrane segments, because they were flanked by fusions with high AP activities (Fig. 1). These results supported our working model. Some of the computer programs for the topology prediction suggested the presence of 11 TMS in the

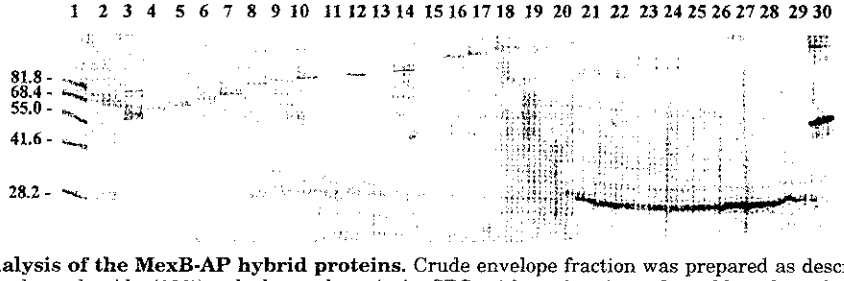

FIG. 2. **Western blot analysis of the MexB-AP hybrid proteins.** Crude envelope fraction was prepared as described under "Experimental Procedures," subjected to polyacrylamide (10%) gel electrophoresis in SDS without heating, electroblotted to the polyvinylidene difluoride membrane and visualized with monoclonal antibody raised against alkaline phosphatase (*lanes 2–20*). Whole cell lysate was subjected to the electrophoresis and stained as above (*lanes 21–27*). The sample was coded by the fusion site. *Lane 1*, molecular weight markers (Western doctor); *lane 2*, Pro^{9}; *lane 3*, Gln^{34}; *lane 4*, Asp^{59}; *lane 5*, Thr^{89}; *lane 6*, Val^{105}; *lane 7*, Arg^{124}; *lane 8*, Ile^{214}; *lane 9*, Gly^{271}; *lane 10*, Thr^{309}; *lane 11*, Glu^{346}; *lane 12*, Leu^{349}; *lane 13*, Thr^{392}; *lane 14*, Phe^{459}; *lane 15*, Thr^{473}; *lane 16*, Asn^{616}; *lane 17*, Leu^{696}; *lane 18*, Gln^{871}; *lane 19*, Ser^{921}; *lane 20*, Gly^{1007}; *lane 21*, Leu^{366}; *lane 22*, Val^{411}; *lane 23*, Gly^{440}; *lane 24*, Arg^{538}; *lane 25*, Pro^{897}; *lane 26*, Pro^{972}; *lane 27*, Gln^{1046}; *lane 28*, pBAD*phoA*; *lane 29*, pMEXB1; *lane 30*, bacterial alkaline phosphatase.

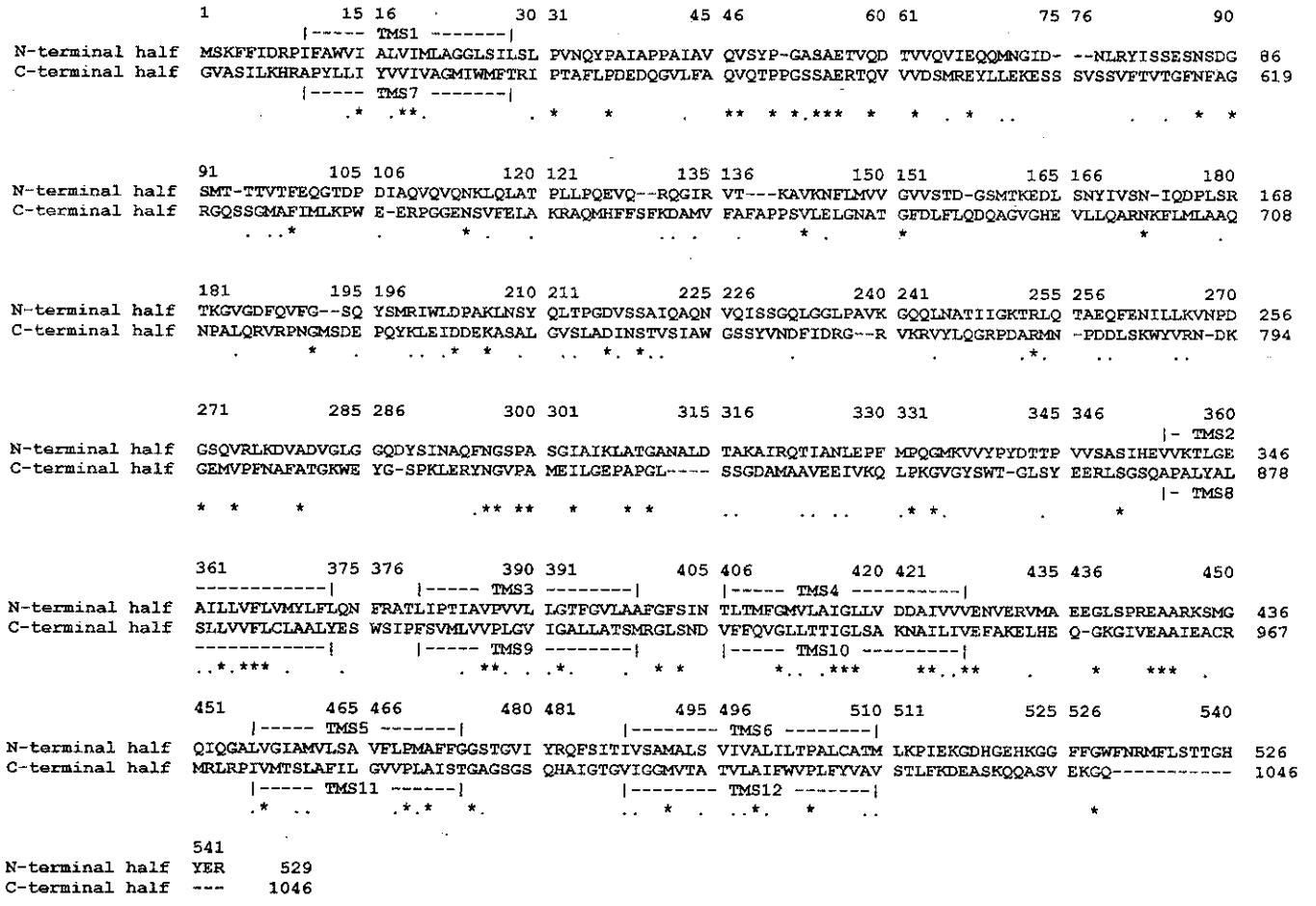

FIG. 3. **Sequence alignment of amino- and carboxyl-terminal halves.** Amino acid sequence of MexB was split into two between residues 529 and 530. Multiple sequence alignment was carried out using the program Clustal W 1.7. The *horizontal dots* indicate the TMS. *Asterisks* and *dots* indicate identical and similar amino acid residues, respectively.

MexB polypeptide. Our results experimentally ruled out this possibility.

We carried out computer-aided alignment analysis of the amino-terminal and carboxyl-terminal halves of the polypeptide from Met^{1} to Arg^{529} and Gly^{530} to Gln^{1046}, respectively. Fig. 3 shows 30% homology between the first and second halves. TMS 1, 2, 3, 4, 5, and 6 of the amino-terminal half could be overlaid by TMS 7, 8, 9, 10, 11, and 12 in the carboxyl-terminal half, respectively. This 2-fold repeat suggested that *mexB* is evolved from an ancestral gene encoding a protein of six TMS by an intragenic duplication as predicted earlier (13, 22). This is to doubly support the transmembrane nature of the segments experimentally assigned to be the membrane-spanning domain. In addition, the distribution of positive charges in the cytoplasmic and periplasmic domains were 22 and 2, respectively, excepting the first and fourth large periplasmic domains with more than 60 amino acid residues (Fig. 1). The result was in accord with the positive inside rule (38).

This is the first experimental verification of the transmembrane topology of the RND family extrusion pump protein. This experimentally verified model has the following features. (i) The MexB protein spans the membrane 12 times leaving amino and carboxyl termini at cytoplasmic side of the inner membrane as suggested for the RND family proteins (13, 22). (ii) MexB has two large hydrophilic segments with 311 and 314 amino acid residues from 29 to 338 (between TMS 1 and 2) and from 558 and 871 (between TMS 7 and 8), respectively. (iii) The membrane topology of MexB appeared to have a 2-fold repeat. These big loops might interact with the periplasmic subunit, MexA, and the outer membrane subunit, OprM. It is conceivable that these large loops transmit cellular energy to the OprM channel gate. In addition, we found 5 charged amino acid residues in the transmembrane domains. These charged residues were highly conserved in the RND family efflux proteins as aligned by the Clustal W multi-alignment software (data not shown). Specific localization of the highly conserved charged residues in the TMS suggested that they might play an important role in substrate binding and proton transport. Further studies are needed to elucidate the role of these amino acid residues in the mechanism of xenobiotics extrusion.

Acknowledgment—We acknowledge the preliminary participation of Weil EL-Naggar in this study.

REFERENCES

1. Brown, M. R. W. (1975) in *Resistance of Pseudomonas aeruginosa* (Brown, M. R. W., ed) pp. 71–107, John Wiley and Sons, London
2. Nakae, T., Yoshihara, E., and Yoneyama, H. (1997) *J. Infect. Chemother* **3,** 173–183
3. Rella, M., and Haas, D. (1982) *Antimicrob. Agents Chemother.* **22,** 242–249
4. Lei, Y., Sato, K., and Nakae, T. (1991) *Biochem. Biophys. Res. Commun.* **178,** 1043–1048
5. Hirai, K., Suzue, S., Irikura, T., Iyobe, S., and Mitsuhashi, S. (1987) *Antimicrob. Agents Chemother.* **31,** 582–586
6. Fukuda, H., Hosaka, M., Hirai, K., and Iyobe, S. (1990) *Antimicrob. Agents Chemother.* **34,** 1757–1761
7. Ramos, J. L., Duque, E., Godoy, P., and Segura, A. (1998) *J. Bacteriol.* **180,** 3323–3329
8. Goldstein, L. J., Galski, H., Fojo, A., Willingham, M., Lai, S. L., Gazdar, A., Priker, R., Green, A., Crist, W., and Brodeur, G. M. (1989) *J. Natl. Cancer Inst.* **81,** 116–124
9. Poole, K., Krebes, K., McNally, C., and Neshat, S. (1993) *J. Bacteriol.* **175,** 7363–7372
10. Moreshed, S. R. M., Lei, Y., Yoneyama, H., and Nakae, T. (1995) *Biochem.*

Biophys. Res. Commun. **210,** 356–362
11. Yoneyama, H., Ocaktan, A., Tsuda, M., and Nakae, T. (1997) *Biochem. Biophys. Res. Commun.* **233,** 611–618
12. Ocaktan, A., Yoneyama, H., and Nakae, T. (1997) *J. Biol. Chem.* **272,** 21964–21969
13. Paulsen, I. T., Brown, M. H., and Skurray, R. A. (1996) *Microbiol. Rev.* **60,** 575–608
14. Dong, Q., and Mergeay, M. (1994) *Mol. Microbiol.* **14,** 185–187
15. Dinh, T., Paulsen, I. T., and Saier, M. H., Jr. (1994) *J. Bacteriol.* **176,** 3825–3831
16. Nikaido, H. (1994) *Science* **264,** 382–388
17. Ma, D., Cook, D. N., Hearst, J. E., and Nikaido, H. (1994) *Trends Microbiol.* **2,** 489–493
18. Srikumar, R., Li, X., and Poole, K. (1997) *J. Bacteriol.* **179,** 7875–7881
19. Gotoh, N., Tsujimoto, H., Nomura, A., Okamoto, K., Tsuda, M., and Nishino, T. (1998) *FEMS Microbiol. Lett.* **165,** 21–27
20. Yoneyama, H., Ocaktan, A., Gotoh, N., Nishino, T., and Nakae, T. (1998) *Biochem. Biophys. Res. Commun.* **244,** 898–902
21. Köhler, T., Michéa-Hamzehpour, M., Henze, U., Gotoh, N., Curty, L. K., and Pechère, J.-C. (1997) *Mol. Microbiol.* **23,** 345–354
22. Saier, M. H., Jr., Tam, R., Reizer, A., and Reizer, J. (1994) *Mol. Microbiol.* **11,** 841–847
23. von Heijne, G. (1992) *J. Mol. Biol.* **225,** 487–494
24. Manoil, C., and Beckwith, J. (1985) *Proc. Natl. Acad. Sci. U. S. A.* **82,** 8129–8133
25. Manoil, C., Mekalanos, J. J., and Beckwith, J. (1990) *J. Bacteriol.* **172,** 515–518
26. Ehrmann, M., Bolek, P., Mondigler, M., Boyd, D., and Lange, R. (1997) *Proc. Natl. Acad. Sci. U. S. A.* **94,** 13111–13115
27. Gutierrez, C., and Devedjian, J. (1989) *Nucleic Acids Res.* **17,** 3999
28. Boyd, D., Traxler, B., and Beckwich, J. (1993) *J. Bacteriol.* **175,** 553–556
29. Guzman, L.-M., Belin, D., Carson, M. J., and Bechwith, J. (1995) *J. Bacteriol.* **177,** 4121–4130
30. Ehrmann, M., Boyd, D., and Beckwich, J. (1990) *Proc. Natl. Acad. Sci. U. S. A.* **87,** 7574–7578
31. Michaelis, S., Inouye, H., Oliver, D., and Beckwith, J. (1983) *J. Bacteriol.* **154,** 366–374
32. Laemmli, U. K. (1970) *Nature* **227,** 680–685
33. Gott, P., and Boos, W. (1988) *Mol. Microbiol.* **2,** 655–663
34. Allard, J. D., and Bertrand, K. P. (1992) *J. Biol. Chem.* **267,** 17809–17819
35. Enomoto, H., Unemoto, T., Nishibuchi, M., Padan, E., and Nakamura, T. (1998) *Biochim. Biophys. Acta* **1370,** 77–86
36. Cole, S. P., Bhardwaj, G., Gerlach, J. H., Mackie, J. E., Grant, C. E., Almquist, K. C., Stewart, A. J., Kurz, E. U., Duncan, A. M., and Deeley, R. G. (1992) *Science* **258,** 1650–1654
37. Fujii, R., Mutoh, M., Niwa, K., Yamada, K., Aikou, T., Nakagawa, M., Kuwano, M., and Akiyama, S. (1994) *Jpn. J. Can. Res.* **85,** 426–433
38. von Heijne, G. C. (1986) *EMBO J.* **5,** 3021–3027

ELSEVIER

FEMS Microbiology Letters 181 (1999) 91–100

FEMS MICROBIOLOGY LETTERS

Cloning and sequences of inducible and constitutive macrolide resistance genes in *Staphylococcus aureus* that correspond to an ABC transporter

Mayumi Matsuoka [a,*], László Jánosi [b], Kikutarou Endou [a], Yoshinori Nakajima [a]

[a] *Division of Microbiology, Hokkaido College of Pharmacy, 7-1 Katsuraoka-cho, Otaru, Hokkaido 047-0264, Japan*
[b] *National Center for Epidemiology, H-1097 Budapest, Gyali ut 2-6, Hungary*

Received 19 July 1999; received in revised form 27 September 1999; accepted 28 September 1999

Abstract

A restriction map was made and the DNA sequence was determined for a plasmid, pMC38, derived from the inducible macrolide resistance plasmid pEP2104, that showed constitutive resistance to PMS antibiotics (partial macrolide and streptogramin B antibiotics). A 5.04 kb *Sal*I-*Pst*I fragment (fragment C) of pMC38, which encoded PMS resistance, was cloned into a shuttle vector, pRIT5, to yield pMR504. The transformant *Staphylococcus aureus* 4220 (pMR504) exhibited constitutive PMS resistance. Fragment C was subcloned to pUC19 in order to determine the DNA sequence. This sequence was consequently found to contain three open reading frames (ORF1–3), of which ORF3 corresponded to the 63 kDa membrane protein (MsrSA) that expressed PMS resistance. According to DNA sequence comparison of the control region of ORF3 in pMC38 and pEP2104, 44 nucleotides including RBS1 and the leader peptide (MTASMRLK) were deleted on plasmid pMC38. This suggests that the leader peptide is essential for the inducible expression of PMS resistance.

Keywords: *msr* gene; Macrolide resistance; Erythromycin resistance; *Staphylococcus aureus*; Active efflux; ABC transporter

1. Introduction

Macrolide antibiotics (Mac) consist of a 12- to 16-membered lactone ring combined with a sugar moiety. They inhibit protein synthesis via binding to 23S ribosomal RNA in bacteria. The 14- and 16-membered Mac are used for treating infectious diseases caused by Gram-positive [1] and other bacteria; e.g. *Haemophilus influenzae*, *Bordetella pertussis*, *Legionella pneumophila*, *Campylobacter*, *Treponema pallidum* and *Mycoplasma* [1–3].

Resistance to macrolide, lincosamide, and streptogramin B (MLS) antibiotics in staphylococci is known to have the following mechanisms: (1) alteration of the target on ribosome due to dimethylation of a specific adenine residue in the 23S ribosomal RNA by the product of the *erm* gene, and consequently a decrease in binding of MLS antibiotics [4–6]; (2) inactivation of streptogramin B (STG-B) and lincosamide by the products of the *sbh* (encoding

* Corresponding author. Tel.: +81 (134) 62-1902; Fax: +81 (134) 62-1902; E-mail: matsuoka@hokuyakudai.ac.jp

0378-1097/99/$20.00
PII: S0378-1097(99)00518-2

streptogramin B hydrolase) [7] and *linA'* (encoding 3-lincomycin 4-clindamycin *O*-nucleotidyltransferase) [8] genes, respectively; and (3) active efflux of Mac and STG-B antibiotics determined by the *msrA* and *msrB* genes in *Staphylococcus epidermidis* and *Staphylococcus xylosus*, respectively [9,10], both of which appear to act as ATP-dependent efflux pumps.

We have shown that *Staphylococcus aureus* 8325(pEP2104) exhibits inducible resistance to PMS [11] (partial macrolide and streptogramin B) antibiotics (the 14-membered macrolides, erythromycin (EM), and oleandomycin (OL), and the 16-membered macrolide mycinamicin (MCM) and STG-B). The sequence of the N-terminal amino acid residues of a 63 kDa protein (MsrSA) that appeared in the membrane of PMS-resistant strains was identical to that of an MsrA polypeptide related to enhanced efflux of [^{14}C]EM [12]. Ribosomes from PMS-resistant strains showed a similar affinity for EM to those from the PMS-sensitive host strain NCTC8325, and no inactivation of EM by 8325(pEP2104) was observed [11].

In the present study, we determined the DNA sequence of the *msrSA* region on the constitutive PMS-resistant plasmid pMC38, PMS-inducible resistant plasmid pEP2104 and PMS-sensitive mutant plasmid pSP6, and we identified the region that is essential for inducible expression in PMS resistance. In addition, we investigated the relationship between PMS resistance and intracellular accumulation of EM.

2. Materials and methods

2.1. Bacteria, vectors, and media

S. aureus strains used in this study were inducible PMS-resistant 8325(pEP2104), constitutive PMS-resistant 8325(pMC38), 8325(pSP6) which is a PMS-sensitive mutant of 8325(pEP2104), susceptible strains NCTC8325 and RN4220 which is an 8325r$^-$ mutant used as a host strain for the shuttle vector pRIT5, and constitutive MLS-resistant 8325(pI258) and inducible MLS-resistant MS13837 which were conferred by the *ermB* and *ermC* genes, respectively. *Escherichia coli* JM109 was used as a host strain for the cloning vectors pUC19 and pRIT5. Shuttle vector, pRIT5, confers ampicillin resistance in *E. coli* and chloramphenicol resistance in *S. aureus*. Brain heart infusion (BHI) and BHI agar (BHIA) media obtained from Becton Dickinson and Company (USA) were used to cultivate bacteria.

2.2. Chemicals

EM, OL, clindamycin hydrochloride (CLDM), chloramphenicol, and tris(hydroxymethyl)aminomethane (Tris) were obtained from Sigma Chemical Co.; MCM and rokitamycin (RKM) were obtained from Asahi-Kasei Co.; ampicillin (sodium) was obtained from Wako Pure Chemical Industries Ltd.; [*N*-methyl-^{14}C]EM (^{14}C-EM: 54.0 mCi/mmol) was obtained from Amersham Japan Co.; and azithromycin (AZM) was obtained from Pfizer Taito Co. Mikamycin B (MKM-B), a streptogramin type B antibiotic, was purified from a mikamycin mixture (obtained from Banyuu Co.) using liquid chromatography. Carbonylcyanide-*m*-chlorophenylhydrazone (CCCP) was obtained from Sigma; Inulin[^{14}C] carboxylic acid 74–370 mBq/mmol, 2–10 mCi/mmol CAF399 was obtained from Amersham; [^{14}C]EM (57.0 mCi/mmol) was obtained from E.I. du Pont de Nemours and Co.; and *N*-(2-hydroxyethyl) piperazine-*N'*-3-propansulfonic acid (HEPES) was obtained from Nacalai Tesque. Other chemicals were purchased from commercial sources. *Bam*HI (10 U μl^{-1}) and *Bgl*II (10 U μl^{-1}) were obtained from TOYOBO, and *Pst*I (12 U μl^{-1}), *Sal*I (20 U μl^{-1}), *Xba*I (20 U μl^{-1}) were obtained from New England Bio Labs.

2.3. Determination of antibiotic susceptibility

The minimum inhibitory concentrations (MICs) of antibiotics were determined on Mueller-Hinton II agar plates by the two-fold dilution method recommended by the Japan Society of Chemotherapy [13]. The 50% inhibitory dose (ID_{50}) was determined as follows: overnight cultures of *S. aureus* were added to a fresh medium H (containing nutrient broth, 0.2% yeast extract, and 50 mM HEPES-Na; pH 7.6) [14] and incubated to log phase. After cells were collected by centrifugation, they were sus-

pended in fresh medium H, mixed with a serial two-third dilution of antibiotics, and incubated at 37°C with gentle shaking. Bacterial growth in the presence (experiment A) and absence (experiment B) of antibiotics was determined turbidimetrically. The ratio of the growth rates in experiments A and B is referred to as the relative inhibition (%). The ID_{50} of antibiotics was determined by probit analysis [15].

2.4. Assay for induction of resistance

The agar disk diffusion test used for resistance induction was the same as that described previously [14].

2.5. Cell volume of S. aureus

Overnight culture of staphylococci was incubated to log phase in fresh medium H. Thirty ml of the culture (an absorbancy of 0.2 at 620 nm) was centrifuged at 2900×*g* for 10 min at 4°C. The pellet was washed with 0.2 M phosphate buffer (pH 7.0) and recentrifuged at 27000×*g* for 3 min at 4°C. The bacteria were suspended in 200 μl of 0.2 M phosphate buffer (pH 7.0), put into a 'cell volume measurement centrifuge tube', and centrifuged at 1700×*g* for 3 min at 4°C. The pellet without the supernatant was regarded as the 'packed cell volume'. A mixture of packed cells and 300 μl of 3% [^{14}C]Inulin was placed on ice for 5 min in a 1.5 ml microtube. After centrifugation at 15000×*g* for 3 min at 4°C, radioactivity of 250 μl of supernatant was measured by a liquid scintillation counter. Calculation of cell volume from [^{14}C]Inulin was performed according to the method of Mizushima et al. [16].

2.6. Intracellular accumulation of EM

An overnight culture of *S. aureus* was incubated in fresh medium H until log phase. After centrifugation, it was suspended in medium H to give an absorbancy of 0.35 at 610 nm and was incubated at 37°C with [^{14}C]EM 1 μg ml^{-1} in an L-tube. Turbidity measurements and sampling of the culture were done at 10 min intervals. One ml samples were passed through a 0.45 μm nitrocellulose membrane filter. Filters were washed with 4 ml of HEPES A buffer (10 mM HEPES, 16 mM $Mg(CH_3COO)_2$, 50 mM NH_4Cl, 1 mM EGTA, and 0.1 mM DTT; pH 7.6) containing 50 μg EM ml^{-1}, and intracellular accumulation of EM was measured by a liquid scintillation counter. In the case of EM induction, the strain was cultivated overnight in the presence of 1.35 μg EM ml^{-1}. CCCP was added to the L-tube after 40 min of incubation.

2.7. Preparation of plasmid DNA

Isolation of covalently closed circular plasmid DNA was performed according to the previously described method [17] except that lysozyme (at a final concentration of 0.82 mg ml^{-1}) was substituted for lysostaphin when plasmids were obtained from *E. coli* cells.

2.8. Cloning of resistance genes

Plasmid pMC38 was digested with restriction enzymes *Pst*I and *Sal*I, and the 5.04 kb fragment (designated as fragment C) of pMC38 was inserted into pRIT5 and transformed into *S. aureus* RN4220 by electroporation (set voltage, 2.5 kV; capacitor, 25 μF; resistor, 200 Ω; time constants, 4.0∼3.8 ms; Bio-Rad Gene Pulser). Following the confirmation of the presence of the resistance gene, fragment C was subcloned – for determination of the DNA sequence – into pUC19 and transformed to *E. coli* JM109 using competent cells prepared by Hanahan's method [18].

2.9. Sequence analysis of DNA nucleotides

Automated fluorescent sequencing was performed on double-strand DNA with an Applied Biosystems Apparatus (model 373A), using a Dye Terminator Cycle Sequencing Ready Reaction Kit (Applied Biosystem Inc., USA). The nucleotide sequences were analyzed in BLASTN. A homology search of deduced amino acid sequences was carried out through the protein databases of NBRF (National Biochemical Research Foundation) and GenBank, using GENETYX-Mac software (Ver. 9.0, Software Development, Japan).

2.10. PCR amplification of the msrSA gene from clinical isolates

To investigate the presence of the PMS-resistant gene in 56 inducible resistant *S. aureus* strains, PCR of the *msrSA* gene was performed using total DNA. Four primers were derived from the nucleotide sequence of the *msrSA* gene that was determined in this study (Accession No. AB016614). Primers specific for the first ATP-binding cassette region of *msrSA* (ABC1F, 5′-ATGGAACAATATACAATTAA-3′ and ABC1R, 5′-ATGATAACTTTGTGGTTTTT-3′: 843 bp) and the second ATP-binding cassette region of *msrSA* (ABC2F, 5′-CGTAGGTGCAAATGGTGTAGG-3′ and ABC2R, 5′-CGATAATTTCGTTCTTTCCCC-3′: 271 bp) were designed. The PCR buffer contained 1.5 mM $MgCl_2$. Nucleotide triphosphates were added at a concentration of 0.2 mM. A total of 2.5 units of *Taq* polymerase was added to 100 μl of reaction mixture. The polymerase

(A) *S. aureus* 8325(pEP2104)

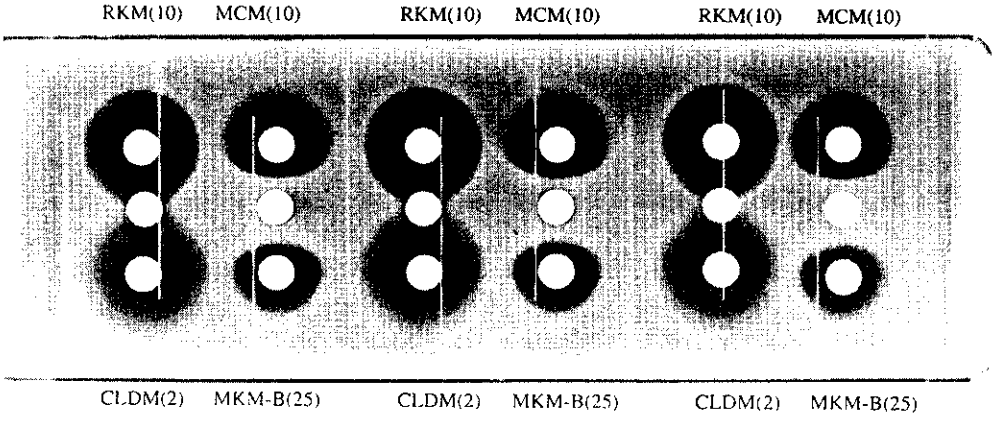

(B) *S. aureus* MS13837

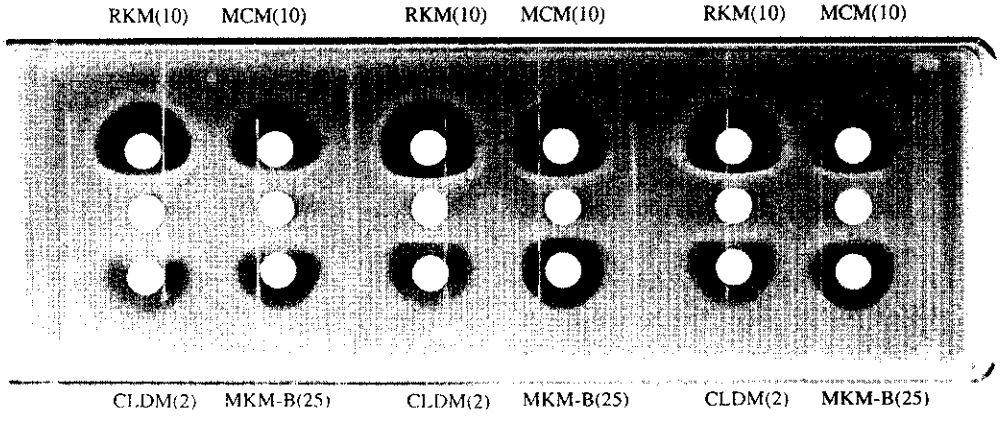

Fig. 1. Effect of erythromycin, oleandomycin, and azithromycin on susceptibility to rokitamycin (RKM), mycinamicin I (MCM), clindamycin (CLDM), and mikamycin B (MKM-B) in *S. aureus* 8325(pEP2104) (A) and MS13837 (B). Disks impregnated with the amount of antibiotics indicated in parentheses (in μg) were placed in the top (RKM and MCM) and bottom (CLDM and MKM-B) rows. In the center row, the two disks on the left contained erythromycin (E), the two disks in the middle contained oleandomycin (O) and the two disks on the right contained azithromycin (A) at 10 μg per disk.

Table 1
50% Inhibitory dose (ID_{50}) of antibiotics against cell growth of *S. aureus*

Strain	ID_{50} (μg ml^{-1})				
	EM	OL	AZM	MCM	MKM-B
NCTC8325	0.07	0.13	0.14	0.04	2.85
8325(pE2104)	3.32	2.04	6.0	0.06	3.47
8325(pEP2104)[a]	11.6	5.67	28.6	0.75	30.3
8325(pMC38)	11.6	5.07	10.5	0.45	17.0
8325(pSP6)	0.05	0.13	0.08	0.07	2.68

Abbreviations: EM, erythromycin; OL, oleandomycin; AZM, azithromycin; MCM, mycinamicin I; MKM-B, mikamycin B.
[a]Induced by 1.35 μg EM ml^{-1}.

reactions were carried out in a Perkin Elmer Gene Amp PCR System 9600 apparatus. The PCR protocol consisted of a 135 s denaturation pulse at 94°C followed by 30 cycles of the following: a 45 s denaturation step at 94°C, a 30 s primer-annealing step at 55°C, and a 90 s extension step at 72°C. The cycle was terminated by a final 10 min incubation at 72°C.

3. Results and discussion

3.1. Susceptibility of PMS-resistant strains

S. aureus PM2104 [14,19], isolated in Hungary in 1977, did not show MLS-type resistance but did show PMS-type resistance, namely resistance to only EM, OL, MCM, and MKM-B, and there was no cross-resistance shown. Plasmid pEP2104 from PM2104 was transduced into the antibiotic-susceptible *S. aureus* NCTC8325 strain. Susceptibility profiles of *S. aureus* 8325(pEP2104) and *S. aureus* MS13837 showing MLS-type resistance by the agar disk diffusion technique are shown in Fig. 1. Phenotypes for Mac resistance in *S. aureus* are classified into three groups [20]: those that show constitutive resistance (group A), those that show EM- and OL-inducible resistance (group B), and those that show only EM-inducible resistance (group C). *S. aureus* MS13837, a strain clinically isolated in Japan, showed EM- and OL-inducible resistance to all Mac, while 8325(pEP2104) showed EM- and OL-inducible resistance to only MCM and MKM-B. We have tried AZM, a new 15-membered Mac, as an inducer, and found that it had inducer activity for inducible PMS- and MLS-resistant strains belonging to group B.

The ID_{50} value of AZM was high in EM-induced 8325(pEP2104) and constitutive PMS-resistant 8325(pMC38) strains, and these strains showed higher values than non-induced 8325(pEP2104) for other drugs as well. Moreover, the ID_{50} values of MCM and MKM-B in the EM-induced 8325(pEP2104) strain (0.75, 30.3 μg ml^{-1}) were higher than that of the 8325(pMC38) strain (0.45, 17.0 μg ml^{-1}) (Table 1). The amount of MsrSA protein in the cell membrane protein that conveys PMS resistance was measured in 20 μg of total cell membrane protein by a densitometer. The measured values were 4.1% in 8325(pEP2104), 14.2% in EM-induced 8325(pEP2104) and 8.0% in 8325(pMC38) (data not shown), although the 63 kDa membrane protein (MsrSA) was almost undetectable in sensitive strains, NCTC8325 and 8325(pSP6). It appears, therefore, that the level of PMS resistance is related to the production of MsrSA protein.

S. aureus 8325(pSP6), which is derived from the inducible PMS-resistant strain 8325(pEP2104) by nitrosoguanidine treatment, showed low ID_{50} for all Mac as well as sensitive strain NCTC8325 (Table 1), though there was no curing of plasmid and it showed the same restriction map to PMS resistance plasmids pEP2104 and pMC38. This suggests that the expression of PMS resistance in plasmid pSP6 is related to the mutation of a few nucleotides, not to the addition or deletion of a certain region.

Table 2
MICs of PMS antibiotics in *S. aureus* and *E. coli*

Strain	Antibiotic (μg ml^{-1})				
	EM	OL	AZM	MCM	MKM-B
S. aureus					
NCTC8325	0.39	0.78	1.56	0.20	3.13
8325(pEP2104)	100	50	100	0.39	3.13
8325(pMC38)	100	50	100	12.5	50
8325(pSP6)	0.39	0.78	1.56	0.20	3.13
RN4220	0.39	0.39	1.56	0.05	1.56
4220(pMR504)	100	6.25	50	12.5	25
E. coli					
JM109	50	>100	3.13	12.5	>100
JM109(pMU504)	50	>100	3.13	12.5	>100

Abbreviations: EM, erythromycin; OL, oleandomycin; AZM, azithromycin; MCM, mycinamicin I; MKM-B, mikamycin B.